ปฏิกิริยาการขจัดน้ำของเอทานอลด้วยตัวเร่งปฏิกิริยาวัฏภาคผสมของอะลูมินา

นายธรรมนูญ อินทร์มะณี

วิทยานิพนธ์นี้เป็นส่วนหนึ่งของการศึกษาตามหลักสูตรปริญญาวิศวกรรมศาสตรมหาบัณฑิต
สาขาวิชาวิศวกรรมเคมี ภาควิชาวิศวกรรมเคมี
คณะวิศวกรรมศาสตร์ จุฬาลงกรณ์มหาวิทยาลัย
ปีการศึกษา 2556

ETHANOL DEHYDRATION REACTION OVER MIXED PHASE ALUMINA CATALYSTS

Mr. Tharmmanoon Inmanee

A Thesis Submitted in Partial Fulfillment of the Requirements
for the Degree of Master of Engineering Program in Chemical Engineering
Department of Chemical Engineering
Faculty of Engineering
Chulalongkorn University
Academic Year 2013

Thesis Title	ETHANOL DEHYDRATION REACTION OVER MIXED PHASE ALUMINA CATALYSTS
By	Mr. Tharmmanoon Inmanee
Field of Study	Chemical Engineering
Thesis Advisor	Associate Professor Bunjerd Jongsomjit, Ph.D.

Accepted by the Faculty of Engineering, Chulalongkorn University in Partial Fulfillment of the Requirements for the Master's Degree

.....Dean of the Faculty of Engineering

(Professor Bundhit Eua-arporn, Ph.D.)

THESIS COMMITTEE

.....Chairman

(Associate Professor Muenduen Phisalaphong, Ph.D.)

.....Thesis Advisor

(Associate Professor Bunjerd Jongsomjit, Ph.D.)

.....Examiner

(Assistant Professor Suphot Phatanasri, D.Eng.)

.....External Examiner

(Ekrachan Chaichana, D.Eng.)

ธรรมนูญ อินทร์มะณี : ปฏิกิริยาการขจัดน้ำของเอทานอลด้วยตัวเร่งปฏิกิริยาวัฏภาคผสมของอะลูมินา. (ETHANOL DEHYDRATION REACTION OVER MIXED PHASE ALUMINA CATALYSTS) อ.ที่ปรึกษาวิทยานิพนธ์หลัก: รศ. ดร. บรรเจิด จงสมจิตร , 77 หน้า.

ตัวเร่งปฏิกิริยาวัฏภาคผสมแกมมา และไคของอะลูมินาที่ถูกเตรียมโดยวิธีโซลโวเทอร์-มอลของสารละลายผสม (โทลูอีน และ 1-บิวทานอล) ถูกนำมาศึกษาผลกระทบของอุณหภูมิการเผา และการปรับปรุงด้วยโมลิบดินัมออกไซด์ ตัวเร่งปฏิกิริยาถูกวิเคราะห์คุณลักษณะด้วยการกระเจิงรังสีเอ็กซ์ การดูดซับทางกายภาพด้วยไนโตเจน กล้องจุลทรรศน์อิเล็กตรอนแบบส่องกราด กล้องจุลทรรศน์อิเล็กตรอนแบบส่องผ่าน และการคายแอมโมเนียด้วยการเพิ่มอุณหภูมิแบบตั้งโปรแกรม ความสามารถของตัวเร่งปฏิกิริยาถูกทดสอบการผลิตเอทิลลีนโดยปฏิกิริยาการขจัดน้ำของเอทานอลในวัฏภาคแก๊สที่ความดันบรรยากาศ และอุณหภูมิระหว่าง 200 องศาเซลเซียส ถึง 400 องศาเซลเซียส การศึกษาพบว่าอุณหภูมิการเผา และการเติมโมลิบดินัมออกไซด์มีผลกระทบต่อความเป็นกรดของตัวเร่งปฏิกิริยา การเพิ่มอุณหภูมิการเผาส่งผลให้ความเป็นกรดลดลง ในขณะที่การเติมโมลิบดินัมออกไซด์ลงบนตัวเร่งปฏิกิริยาวัฏภาคผสมของอะลูมินาให้ความเป็นกรดเพิ่มขึ้น โดยเฉพาะอย่างยิ่งความเป็นกรดปานกลางถึงกรดแก่ ในการศึกษานี้ ความสามารถของตัวเร่งปฏิกิริยาของการขจัดน้ำของเอทานอลไปเป็นเอทิลลีนปรากฏชัดเจนว่าขึ้นอยู่กับความเป็นกรดปานกลางถึงกรดแก่ ตัวเร่งปฏิกิริยาวัฏภาคผสมของอะลูมินาที่ถูกเผาที่อุณหภูมิ 600 องศาเซลเซียส (C50-600) ให้ความสามารถของตัวเร่งปฏิกิริยาสูงที่สุด และตัวเร่งปฏิกิริยาที่ปรับปรุงด้วยโมลิบดินัมถูกส่งเสริมให้เกิดปฏิกิริยาการขจัดไฮโดรเจน

ภาควิชา วิศวกรรมเคมี ลายมือชื่อนิสิต .....

สาขาวิชา วิศวกรรมเคมี ลายมือชื่อ อ.ที่ปรึกษาวิทยานิพนธ์หลัก .....

ปีการศึกษา 2556

5570227521 : MAJOR CHEMICAL ENGINEERING
KEYWORDS: MIXED PHASE ALUMINA / ETHYLENE / ETHANOL DEHYDRATION

THARMMANOON INMANEE: ETHANOL DEHYDRATION REACTION OVER MIXED PHASE ALUMINA CATALYSTS. ADVISOR: ASSOC. PROF. BUNJERD JONGSOMJIT, Ph.D., 77 pp.

The mixed gamma and chi crystalline phase alumina catalyst prepared by the solvothermal method of the mixed solution (toluene and 1-butanol) was investigated for the effect of calcination temperatures and MoO_3 modification. The catalysts were characterized by X-ray diffraction (XRD), N_2 physisorption, scanning electron microscopy (SEM), transmission electron microscopy (TEM) and NH_3-tempearture programmed desorption (NH_3-TPD). The catalytic activity was tested for ethylene production by dehydration reaction of ethanol in gas phase at atmospheric pressure and temperature between 200°C to 400°C. It was found that the calcination temperature and MoO_3 loading have an effect on acidity of the catalysts. The increasing in calcination temperature resulted in decreased acidity while the MoO_3 loading on the mixed phase alumina catalyst yielded increased acidity especially medium to strong acid. In this study, the catalytic activity of ethanol dehydration to ethylene apparently depends on the medium to strong acid. The mixed phase alumina catalyst calcined at 600°C (C50-600) gave the highest catalytic activity and the MoO_3 modified catalysts promoted dehydrogenation reaction.

Department: Chemical Engineering Student's Signature .....
Field of Study: Chemical Engineering Advisor's Signature .....
Academic Year: 2013

ACKNOWLEDGEMENTS

I would like to express my sincere thanks to my thesis advisor, Associate Professor Bunjerd Jongsomjit, Ph.D. for his invaluable help and constant encouragement throughout the course of this research. I am most grateful for his teaching and advice. This thesis would not have been completed without all the support that I have always received from his.

In addition, I am grateful for chairman of the committee, Associate Professor Muenduen Phisalaphong, Ph.D and members of the examining committee, Assistant Professor Suphot Phatanasri and Dr. Ekrachan Chaichana, D.Eng., for suggestions and their spending time in reviwe my thesis.

Sincere thank is given to the Thailand Research Fund (TRF) and department of chemical engineering at Chulalongkorn University for the financial support of this work.

Finally, I most gratefully acknowledge my parents and my friends in Center of Excellence on Catalysis and Catalytic Reaction Engineering for all their support throughout the period of this research.

CONTENTS

Page

Page

Page

TABLES CONTENTS

Page

FIGURES CONTENTS

Page

Page

CHAPTER I

INTRODUCTION

1.1 General introduction

Ethylene is intermediate in the petroleum industry. It is produced from crude oil and used as feedstocks to produce a variety of polymers in petrochemical industry such as polyethylene, polyvinyl chloride and polystyrene. Therefore, the demand of ethylene is continued increase. Moreover, ethylene is used as the precursor for synthesis of ethylene oxide, ethylene dichloride, ethylbenzene and so on [1-4]. Traditionally, ethylene is obtained from the thermal catalytic cracking upon an endothermic reaction requiring high temperatures (600°C-1000°C) [1]. However, at present with the rapid development and economic growth, which lead to an enhancement of ethylene production, the crude oil as the raw material is a nonrenewable resource and limit to consume. Therefore, the new suitable ways to produce ethylene instead of crude oil petroleum is considered [5]. The dehydration of alcohol has been considered as promising alternative approach to produce ethylene. The production of ethylene from ethanol is “green chemical technology”. It converts ethanol obtained from renewable biomass such as sugar cane and corn to ethylene.

Dehydration of ethanol over solid acid catalysts requires lower temperature compared to the thermal cracking (600°C-1000°C), leading to the reduction energy cost. So, many researchers have developed the ethanol dehydration for producing ethylene by using solid catalysts. The main product from this reaction is ethylene, whereas diethyl ether (DEE), acetaldehyde and light olefins are byproducts. Each of products is produced at the different temperature for example the high temperature (400°C-450°C) is suitable for produced ethylene, while the byproduct is gained at lower temperature (< 300°C). Besides the reaction temperature, the acidity of the

catalysts is one of the important factors that affected the ability of this reaction. Many researchers have reported that the acid nature of solid catalyst has direct influence on the dehydration activity. The common solid catalysts such as zeolite [1, 6, 7] and alumina (Al_2O_3) [2] have been applied to study the effect of acidity of catalyst on the dehydration ability. Lu et al. (2011) [6] found that HZSM-5 zeolite catalyst exhibits the highest selectivity of ethylene when it was carried out at low temperature (200°C–300°C). However, due to the higher acidity of HZSM-5, it is the disadvantage for dehydration. The acidity of catalyst leads to the formation of coke on the solid support that causes the lower stability. Previous works have been reported that not only acidity strongly affected the dehydration ability, but also influenced on the reaction stability of catalyst. For γ-Al_2O_3 catalyst, the dehydration reaction must be applied at higher temperature (400°C-450°C) to achieve high activity. Therefore, many attempts have been tried to modified γ-Al_2O_3 by adding metal oxide on solid support such as titanium oxide and iron oxide [8, 9]. Chen et al. (2007) found that the modification of γ-Al_2O_3 with TiO_2 can improve acidity. The conversion of ethanol is reached to 99.96%, whereas ethylene selectivity is about 99.4% at 440°C. Although, the modified γ-Al_2O_3 catalyst is required higher temperature than HZSM-5 zeolite catalyst, the γ-Al_2O_3 catalyst is easy to synthesize and the stability of modified γ-Al_2O_3 catalyst is higher.

The γ-Al_2O_3 catalyst is captivating because of its excellent thermal stability, fine particle size, high surface area and inhibit side reaction. Khom-in et al. (2008) [10] studied the synthesis of mixed γ- and χ- phase Al_2O_3 catalysts and applied for methanol dehydration. They reported that the acidity of mixed γ- and χ- phase Al_2O_3 is higher than γ-Al_2O_3 and χ-Al_2O_3 [11-13]. The mixed γ- and χ- phase Al_2O_3 catalysts can be synthesized directly by using the solvothermal method via suitable solvent in order to control structures, grain sizes and morphologies by varying process conditions.

In this research, we focused to develop the alumina-based solid acid catalysts for ethanol dehydration. The catalysts were synthesized, characterized and tested at a specified reaction condition. The synthesis parameters and reaction

conditions influencing on dehydration reaction was varied in order to explore the suitable catalysts and conditions for ethanol dehydration.

1.2 Research objectives

- To study the characteristics and catalytic properties of modified alumina catalysts with for ethanol dehydration reaction to ethylene.
- To investigate yield of ethylene by using modified alumina catalysts obtain highest yields.

1.3 Research scopes

- Investigation the effect of calcination temperature on mixed γ- and χ-crystalline phase catalysts in 50:50 ratio via solvothermal method.
- Investigation the amount of metal oxide (MoO_3) loading over mixed γ- and χ-crystalline phase alumina catalysts. The metal oxide is varied from 0 to 20 wt% of metal.
- Characterization of the catalysts by the following method;
  - The catalyst structures and crystallinity are characterized by X-ray diffraction (XRD)
  - The morphology and crystallite size of all catalysts are characterized by Scanning Electron Microscopy (SEM) and Transmission Electron Microscopy (TEM).
  - The surface area, pore volume and pore size diameter are characterized by N_2 physisorption (BET).
  - The acidity of catalysts is characterized by NH_3-temperature programmed desorption (NH_3-TPD) and ion-exchange/titration.

- Investigation the catalytic performance of all catalysts in ethanol dehydration reaction under atmospheric pressure and temperatures between 200°C to 400°C.

1.4 Research methodology

Research methodology is as shown;

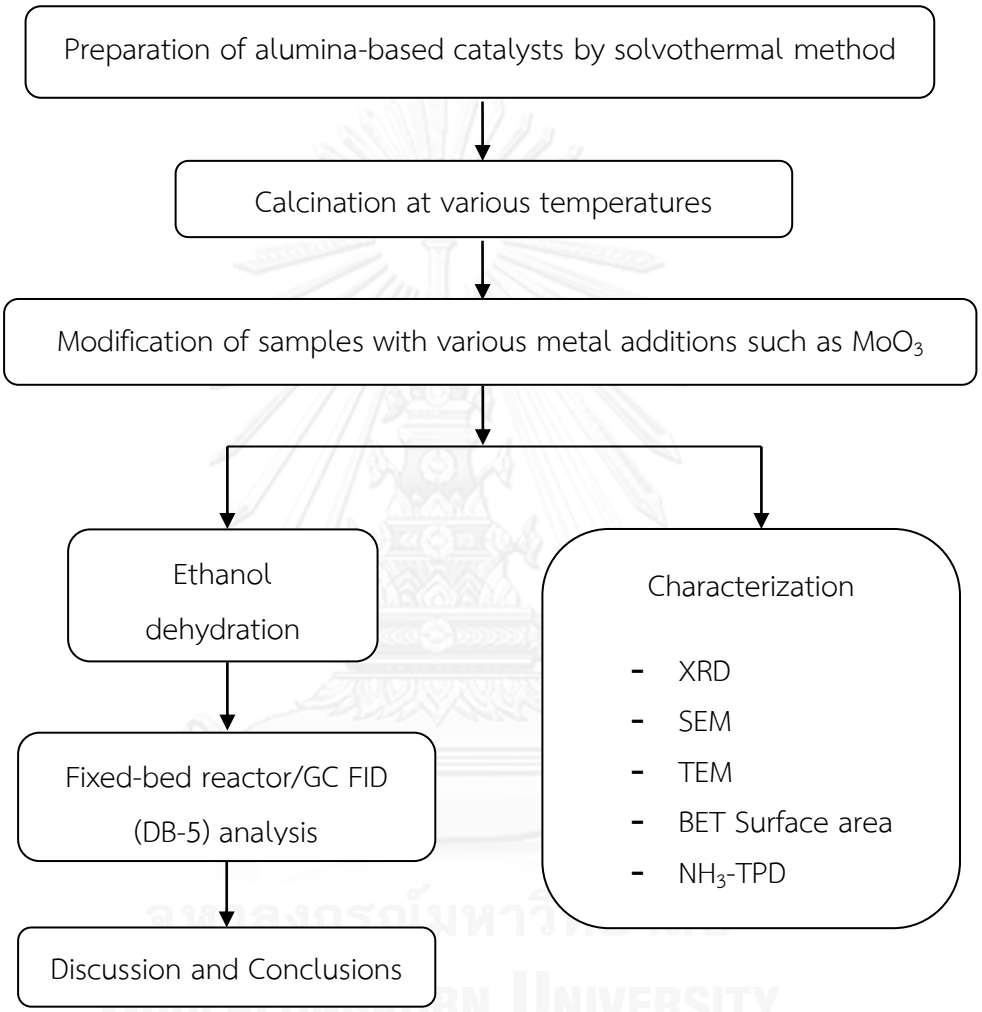

As mentioned above, it explains about the motivation of the research, the research scopes, and the research methodology. Henceforth, the content of thesis is arranged as follow:

Chapter II contains basic knowledge of ethanol dehydration reaction and the catalysts use in ethanol dehydration reaction, including the literature reviews.

Chapter III describes the experimental procedure for catalysts preparation, procedures for reaction testing, and instrument for characterization.

Chapter IV exhibits results and discussion about the effect of calcination temperature and metal loading.

Finally, Chapter V reveals overall conclusion and recommendation of this thesis.

CHAPTER II

THEORY AND LITERATURE REVIEWS

The benefit of ethanol is well known as a solvent. However, it is able to produce a variety of products such as ethylene, diethyl ether (DEE), acetaldehyde, styrene and etc. Ethylene is produced through dehydration reaction of ethanol by using acid catalyst. The basic knowledge of ethanol dehydration reaction and the catalysts used are reviewed as follows in Chapter II.

2.1 Ethanol dehydration reaction

Ethanol consists of hydroxyl group in molecule. It can be dehydrated by using acid catalysts. The hydroxyl group is converted into water molecule. After the water molecule is emitted from ethanol molecule, the hydrocarbon rearranges into ethylene or DEE [14]. The reaction temperature used is between 180 to 500°C in gas phase and liquid phase [15]. The chemical equation of ethanol dehydration reaction is shown in equations (1) and (2) as follows;

$$C_2H_5OH \longrightarrow C_2H_4 + H_2O \qquad +44.9kJ/mol \quad (1)$$

$$2C_2H_5OH \longrightarrow C_2H_5OC_2H_5 + H_2O \qquad -25.1kJ/mol \quad (2)$$

Equation (1) reveals that the reaction of ethanol to ethylene is endothermic reaction. It requires high temperature. In contrast, equation (2) shows that the reaction of ethanol to DEE, which is occurred at the low temperature because the reaction is exothermic. Besides, acetaldehyde is by-product. It is formed at high temperature. Earlier, the catalytic dehydration of ethanol has been improved at which the catalyst can potentially produce ethylene at low temperature leading to

reduction of energy cost of production, while the side reaction (by-products of DEE and acetaldehyde) is favored at low temperature. Thus, the selectivity of ethylene needs to be enhanced.

Nowak and Ziolek (1999) [16] reported the ethanol dehydration reaction required the acid catalyst consisting of the Brønsted acid site on surface of catalyst combining with hydroxyl groups. It generates a water molecule, which is emitted. The mechanism of ethanol dehydration reaction to ethylene is shown as follows in **Figure 2.1**

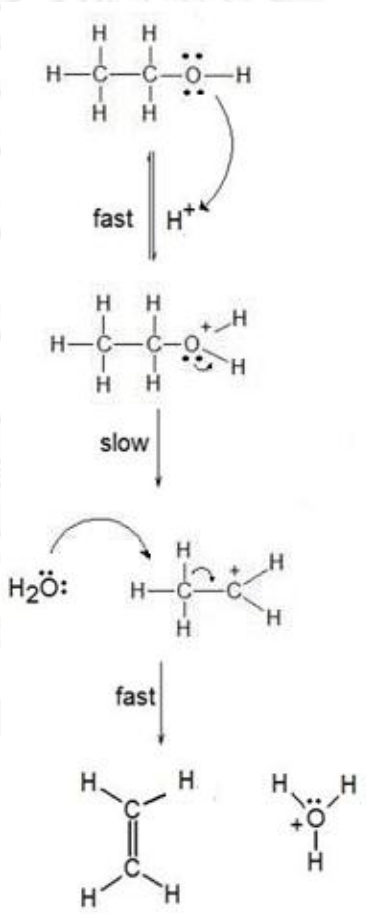

Figure 2.1 The mechanism of ethanol dehydration reaction to ethylene [14].

The mechanism in **Figure 2.1** shows that ethanol dehydration to ethylene is elimination reaction type E1. The E1 reaction is divided into 3 steps [3] as described below:

Step 1: The hydroxyl group in ethanol molecule is leaving group, when proton from acid catalyst adds into the alcoholic oxygen, it makes a better leaving group. This process is so called "protonation". The lone pairs on the oxygen make it a Lewis base. This step is able to be reversible and very fast.

Step 2: Breaking of the C-O bond is endothermic. It causes the loss of the good leaving group (a water molecule) resulting in a carbocation intermediate. This is slow step or the rate determining step.

Step 3: The conjugate base (a water molecule) deprotonates in methyl group leading to the rearrangement of the C=C bond.

In addition, the product of the ethanol dehydration is not only ethylene, but DEE is also able to be produced. In earlier study, many researchers attempt to understand the mechanism of ethanol to DEE, but it cannot be predicted. However, they can find that the alkoxide is an important intermediate of the ethanol to ether [4]. The mechanism of ethanol to DEE is substitution reaction. The generation of DEE explains the reaction mechanism by substitution nucleophilic unimolecular reaction (S_N1) or substitution nucleophilic bimolecular reaction (S_N2) [17].

Zhang and Yu (2013) [4] explain the mechanism of ethanol to DEE by ethylene reaction. This is rate determining step. In the second step, the carbocation associated with nucleophiles is created to DEE compound, which is very fast step.

For the S_N2 reaction, the lone pair electrons of nucleophiles attack the electrophilic electron deficient central atom creating the intermediate. At the same time water molecule is lost and rearrangement to DEE compound. The S_N2 reaction

does not create the carbocation. The mechanisms of ethanol to DEE in the S_N1 and S_N2 reaction are displayed in **Figures 2.2** and **2.3**, respectively.

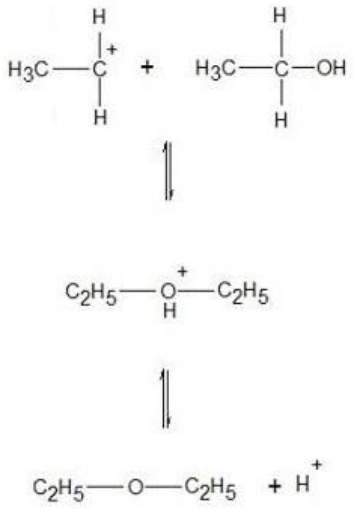

Figure 2.2 The mechanism of ethanol dehydration to DEE in the SN_1 reaction.

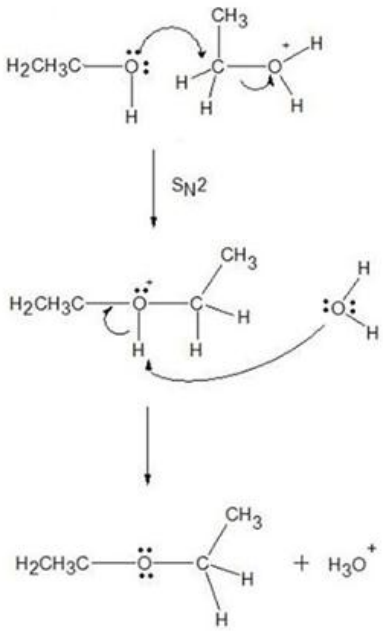

Figure 2.3 The mechanism of ethanol dehydration to DEE in the SN_2 reaction [17].

2.2 Aluminum oxide

2.2.1 Property of aluminum oxide

The structure of aluminum oxide consists of morphology and crystalline structure. The general form is Al_2O_3. The approximate surface areas are about 100 to 600 m^2/g. These properties depend on the synthesis method, water desorption, impurity and heat treatment. There are many phases of aluminum oxide as remarked with Greek alphabet as follows: beta phase (β-Al_2O_3), gamma phase (γ-Al_2O_3), eta phase (η-Al_2O_3), chi phase (χ-Al_2O_3), kappa phase (κ-Al_2O_3), delta phase (δ-Al_2O_3), theta phase (θ-Al_2O_3) and alpha phase (α-Al_2O_3). Each is a unique crystal structure and properties. The phase of aluminum oxide depends on calcined temperatures of reactant (gibbsite, boehmite, and etc.) [11]. For instance, gibbsite is calcined at 280°C to 650°C to obtain chi phase. When it is calcined at 750°C to 1150°C, it obtains the kappa phase alumina. Boehmite is calcined at 480°C to 780°C to obtain the gamma phase. Then, when it was calcined at 780°C to 920°C, it obtains the delta phase. The calcined temperature of aluminum hydroxide is shown in **Figure 2.4.**

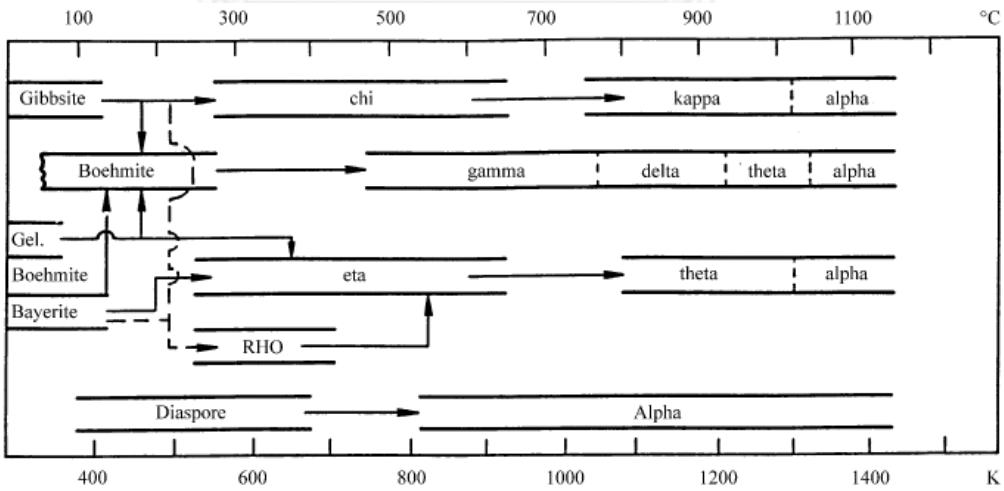

Figure 2.4 The temperature transformation sequence of aluminum hydroxide.

The surface of aluminum oxide contains acid and basic sites. The acid site on surface is Lewis and Brønsted acid site. It is received from Al^{3+} ion and water molecule coordinated with cation, while the basicity on surface is derived from basic hydroxide group and O^{2-} anion.

When aluminum oxide contacts with humidity, the water molecule has adsorbed on surface aluminum oxide and dried in air at temperature between 100°C to 150°C, the water molecule is emitted, but remains hydroxyl group on surface alumina. The role of hydroxyl group is Brønsted acid site as shown in **Figure 2.5.** The acid strength and concentration of aluminum oxide are low when calcined below 300°C, while calcination at 500°C decreases Brønsted acid site. The calcination temperature above 600°C results in adjacent hydroxyl group form into water molecule. Then, the water molecule releases and appears as Al^{3+} ion on surface, which is Lewis acid site [18] as illustrated in **Figure 2.6.**

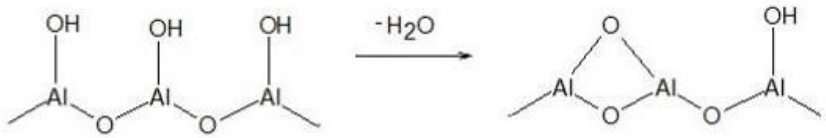

Figure 2.5 Water desorption on surface aluminum oxide.

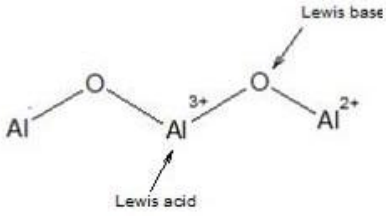

Figure 2.6 Lewis acid site on surface aluminum oxide.

2.2.2 Synthesis of aluminum oxide: the solvothermal method

Aluminum oxide can be prepared with various technique; sol–gel [19, 20], hydrothermal and sovolthermal methods [10, 12, 13, 21]. Usually, aluminum oxide is synthesized by calcination of suitable reactants but this method requires high thermal and difficult control particle size. The precipitation method is complexity and long synthesis times (washing times and aging time). Usually, metal alkoxide used as precursors for produce aluminum oxide via the sol-gel method. However, the limitation of sol-gel method is long gelation periods and high prices of alkoxide. The hydrothermal is very similar to the solvothermal method. It is difference precursor in first step, the aqueous solution used as precursor in the hydrothermal method while the solvothermal method is usually not aqueous (but this is not always).

The “solvothermal” method is a synthesis of inorganic compounds form organic compounds at temperatures between 200°C to 300°C under autogenous pressure of the organics. When upon suitable organic compounds such as ethanol, 1-butanol, toluene, and etc. in order to control structures, grain sizes, shape distribution and morphologies by varied process conditions: reaction temperature, reaction time, solvent type, and precursor type. The prefix “solvo-” means any type of solvent for example alcohol is used as the reaction media, the reactions is called “alcohothermal” reactions.

Generally, the definition of the solvothermal method is reactions at temperatures higher than the boiling point of the intermediary in liquid or supercritical media. The reaction is carried out in closed system using autoclaves, an apparatus shown in **Figure 2.7**

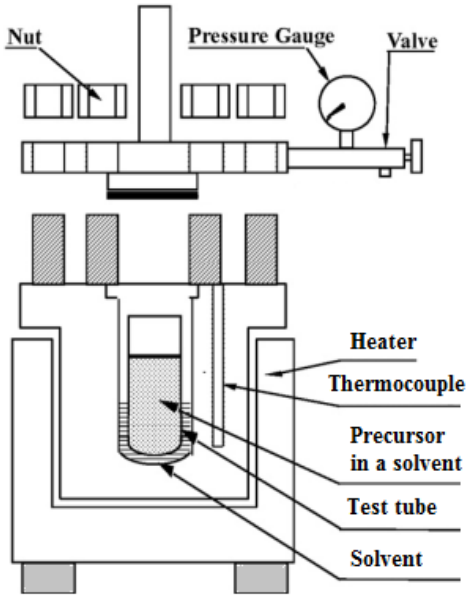

Figure 2.7 Autoclave reactor for solvothermal method [21].

2.3 Molybdenum trioxide

The formula of molybdenum trioxide is MoO_3. The oxidation state of compound is +6. The colour is appearance yellow or light blue solid. The solid structure, molybdenum trioxide consist MoO_6 octahedra structure in orthorhombic crystal which MoO_6 octahedra coordinate cross-linked by oxygen atom. The MoO_3 structure as shown in **Figure 2.8**

Mo is an interesting heterogeneous catalyst for a variety of catalytic reaction such as selective oxidation of alkane, alkene and alcohols. Many researcher [22-24] have been investigated physical and catalytic properties, the oxidation state of Mo species is an important on the surface acidity and catalytic activity. Eric et al. (1995) [25] was studies surface acidity of Rh-Mo/Al_2O_3 catalyst, it was found that when increasing from 2.5 to 3.4% Mo loading to the alumina surface can be increasing amount NH_3, the result indicate that acidity increase relate with amount of Mo. Furthermore, The Mo species on the surface of HZSM-5 catalyst was easier to be

reduced, the reduce of Mo species caused the reduce of acidity of HZSM-5, which is reason to activity drop. However, Mo is able to resistance coke deposit on surface of HZSM-5 [26].

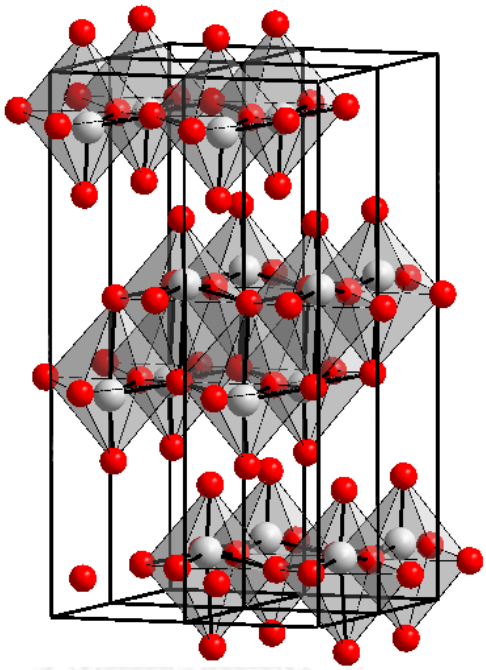

Figure 2.8 The crystal structure of molybdenum trioxide; molybdemum atom (●) and oxygen atom (●).

2.4 Literature rewiews

2.4.1 Catalysts in ethanol dehydration reaction

The acidity of catalyst is important for the ethanol dehydration reaction to ethylene. Many researchers have investigated to improve and develop the catalyst for many years. In first study (1930), the dehydration of ethanol is used phosphoric acid. Later, Pan (1986) [27] studied clay and coke supports loaded phosphate. Pearson et al. (1981) [28] studied parameters for reaction such as ethanol concentration, reaction temperature, space velocity, and life span of catalyst. The

advantages of phosphoric acid catalyst were high ethylene yield. However, the catalysts were rapid deactivated by carbon deposition on surface of catalyst.

The gamma alumina is used in ethanol dehydration to ethylene. It was found that gamma alumina deactivated slowly compared with clay. However, clay provides ethylene yield higher than that obtained from gamma alumina. Zhang et al. (2008) [29] studied gamma alumina used in ethanol dehydration at 475°C that gave ethylene selectivity to 90.1%, while the gamma alumina promoted with TiO_2 increased ethylene selectivity about 99.4% at 500°C as reported by Chen et al. (2007) [9]. Although, the ethanol dehydration to ethylene using gamma alumina obtained activity better than phosphoric acid catalyst, it required high temperature.

The HZSM-5 zeolite is also used as a catalyst in the ethanol dehydration reaction. When compared HZSM-5 with gamma alumina, it rendered higher selectivity of ethylene and ethanol conversion than gamma alumina, while the lower reaction temperature than gamma alumina [5-7, 9, 30, 31] is required. The acidity and pore of HZSM-5 catalyst are important role for hydrocarbon forming [32]. However, the acidity of catalyst leads to coke formation on surface resulting in decreased catalytic activity and short life span. The addition of metal can improve the acidity of HZSM-5 catalyst for ethanol dehydration to ethylene such as lanthanum (La) [7], iron (Fe) [6], and phosphorus (P) [5, 30]. Ramesh et al. (2010) [30] have reported that when phosphate was added into HZSM-5 catalyst, the acidity and resistant carbon deposition on surface of HZSM-5 are increasing, while the selectivity of ethylene does not change. For lanthanum addition, the increased acidity improved catalytic activity at low temperature. Zhan et al. (2010) [33] have investigated La and P-modifiled HZSM-5 catalyst and found that 0.5%La and 2%P exhibited optimum composition, which obtained 99.9% ethylene selectivity and 100% ethanol conversion at 240°C. Han et al. (2011) [26] has been studied the effect of calcination temperature on structure of 5wt% Mo/HZSM-5 catalysts in the catalytic performance of the ethanol dehydration to ethylene, the result was exhibit the acidity decreased with increase of calcination temperature. The calcination

temperature at 500°C was the highest catalytic performance. In addition, the result found that the addition Mo 5wt% over HZSM-5 was decreasing total acidity because Mo species may be interaction with Brønsted acid site. Although, the total acidity decrease, the weak and medium acid site are increasing while strong acid is immediate decreasing.

Mactachowski et al. (2012) [34] investigated the $Ag_3PW_{12}O_{40}$, heteropolyacid catalysts used in ethanol dehydration to ethylene. It was found that the humidity had effect on the catalytic activity. Ethanol conversion increased from 70% to 100%, while the selectivity of ethylene decreased from 100% to 80% with increasing the humidity from 2% to 10% at 200°C. Besides, Hornandez et al. (2013) [35] has been studied the acid-base properties of heteropoly acid in the secondary alcohol dehydration reaction. Using 20wt% heteropoly acids (HPAs) with difference supported calcined at 400, it was found that the reaction mechanism of alcohol dehydration depend on the acid-base properties. The MoP sample presented a 21.2 mol% conversion at 200°C in propan-2-ol, the all products are propylene (87.2 mol%), acetone (8.8 mol%) and di-isopropill ether (DIPE) (4 mol%). The results showed the reaction not only presented dehydration, but also present dehydrogenation which is cause formation of acetone. It bring about summary the Mo besides dehydrating the alcohol exhibit dehydrogenation or oxidation (Oxygen present in system).

From above, the catalysts for ethanol dehydration reaction to ethylene can be divided into 4 group [3, 4] as follows:

- Phosphoric acid catalyst
- Oxide catalyst
- Molecular sieve catalyst
- Heteropolyacid catalyst

However, γ-Al_2O_3 is mostly used as a support for catalysts because its high thermal stability, physical and chemical properties having especially appropriate high surface area and porosity.

2.4.2 Modify gamma-Al_2O_3

The gamma alumina is used as both catalyst and support in a variety of reactions such as hydrogenation, reforming, hydrotreating including dehydration of ethanol. Many researchers have efforts to improve the catalyst for ethanol dehydration reaction. Kwak et al. (2011) [36] studies property of Lewis acid and Brønsted acid on surface aluminum oxide in face 100. It was found that the both Lewis acid site and Brønsted acid site are active center for ethanol dehydration reaction, these depend on calcination temperatures. While Ello et al. (1997) [37] have been reported behavior of acidity on alumina surface as functions of the calcination temperatures, the moisture is lost during the calcination but it easily recovers on the surface alumina. The adsorbed moisture can converse Lewis acid sites to Brønsted acid sites. Although, Lewis acid site is converse, the amount of acidity cannot change. Besides, the different calcination condition can control physical and chemical properties of transition alumina has been reported by Simoni et al. (2013) [38], they was investigated the effect of calcination condition of transition alumina catalyst using statistical experimental design. It was found that the higher pore volume and larger pore size diameters favor the formation with high heating rate. Moreover, the concentration of acid site exhibited high with the short calcination time and high heating rate.

Mollavail et al. (2009) [39] reported that when increasing ratio of mixed alumina and silica, the acidity of catalyst was increased and exhibited higher activity than gamma alumina. Moreover, the addition of metal oxide such as niobium oxide (Nb_2O_5) [39], titanium oxide (TiO_2) [9] and molidinum oxide (MoO_3) [23] can improve acid property of gamma alumina. Shishido et al. (2010) [39] and Teramura et al. (2013) [23] found that Nb_2O_5 and MoO_3 added into gamma alumina at high

calcination temperatures (800°C-900°C) enhance Brønsted acid site, which exhibited the highest Brønsted acid site with 16 wt% of Nb_2O_5 at 850°C and 11 wt% of MoO_3 at 800°C. Abello et al. (2003) [24] has been studied characterization of 13wt% MoO_3/Al_2O_3 modified with Li in propane oxidation dehydrogenation. Addition Li into MoO_3/Al_2O_3, the Li occupy Brønsted acid site and decrease in propane conversion. The MoO_3/Al_2O_3 without Li loading exhibited the highest conversion and rate ratio between dehydration and dehydrogenation rate. Carrier et al. (2003) [22] investigated the preparation of alumina-supported Mo catalysts by incipient wetness impregnation. It was found that the $(NH_4)_3[Al(OH)_6Mo_6O_{18}]$ on Al_2O_3 increase formation and crystallization with long oxide/water contact times (ageing), this compound conduce to MoO_3 formation after calcination. In contrast, short oxide/water contact times (freeze-drying) after impregnation limited MoO_3 formation after calcination because the $(NH_4)_3[Al(OH)_6Mo_6O_{18}]$ compound on Al_2O_3 inhibits with freeze-drying method.

From the previous work, the improvement for acidity of gamma alumina is not only by added metal oxide to gamma alumina, but also synthesis of the mixed phase alumina. Khom-in et al. (2008) [10] reported the synthesis of mixed phase between gamma and chi alumina by the solvothermal method that can increase acidity of gamma alumina. The molar ratio of 20:80 for chi:gamma exhibited the highest acidity. The solvothermal synthesis can control the structure and crystallite size of alumina [12]. The preparation of catalyst by solvothermal method using toluene as solvent can obtain chi phase [44] while mixed solution of 1-butanol and toluene solution can obtain mixed phase alumina between gamma and chi phase with ratio of solvent.

CHAPTER III

EXPERIMENTAL

This chapter explains the laboratory procedures, including the catalyst preparation of mixed γ- and χ-crystalline phase alumina presented in section 3.1, the experimental for ethanol dehydration reaction presented in section 3.2 and the characterization of catalyst are presented in 3.3, respectively.

3.1 Catalyst preparation

The mixed phase alumina was prepared by the solvolthermal method and the mixed phase alumina was modified by impregnation method.

3.1.1 Chemicals

Table 3.1 The chemicals used in the catalysts preparation.

Chemical	Supplier
Aluminum isopropoxide :AIP (98%) $[(CH_3)_2CHO]_3Al$	Aldrich
Toluene (99%)$C_6H_5CH_3$	Merck
1-Butanol (99%) $C_4H_{10}O$	Merck
Methanol CH_3OH	Merck
Ultra high purity nitrogen gas (99.99%)	TIG
Ammoniumheptamolybdate-Tetrahydat $(NH_4)_5Mo_7O_{34}\bullet 4H_2O$	Merck

Table 3.1 is shown the list of chemicals used in the preparation of catalysts.

3.1.2 Synthesis of mixed phase alumina catalysts

Mixed γ- and χ-crystalline phase alumina catalyst were prepared by the solvothermal method, according to the procedure described in ref. [5,6]. Approximately 25g of aluminum isopropoxide (AIP) was suspended in 100ml of mixed solution (50ml toluene + 50ml 1-butanol) in a test tube. Then it was placed in a 300ml autocalve and purge with nitrogen, in the gap between the test tube and the autoclave wall, additional 30ml of same solvent. The mixture was heated to 300°C at heating rate of 2.5°C/min and holding for 2h. After the mixture was cooled down to room temperature, the resulting powders were washed with methanol by several times using centrifusing and dried in air. The obtained powders were calcined in a tube furnace with various temperatures (400°C, 600°C, 800°C and 1000°C) with a heating rate of 10°C/min and holding in air for 6h.

3.1.3 Preparation of MoO_3 modified mixed phase alumina catalysts

The MoO_3 modified mixed phase alumina catalysts were prepared by impregnation of mixed phase alumina with an aqueous solution of ammonium heptamolybdate-tetrahydat [$(NH_4)_5Mo_7O_{34}\bullet 4H_2O$] with various loadings of MoO_3 (5, 10, 15, and 20wt%).The procedure for preparation catalyst as mentioned above was calculated based on 1g of catalyst used. First, ammonium heptamolybdate-tetrahydat was dissolved in deionized water. Then, the solution was added dropwise into approximately 1g of support. The obtained catalyst was dried in air at room temperature for 24 h, dried in oven at 110°C for 6h and calcined in air at 500°C for 2h, respectively.

3.2 Catalyst characterization

3.2.1 X-ray diffraction (XRD)

The bulk crystal structure and X-ray diffraction (XRD) patterns of the catalysts were determined by the SIEMENS D5000 X-ray diffractometer connected with a personal computer with Diffract ZT version 3.3 programs for fully control of the XRD analyzer. The experiment was carried out by using Cu K_α radiation source with Ni filter in the 2θ range of 20 to 80° with a resolution of 0.02°.

3.2.2 Nitrogen physisorption

The BET surface area, pore volume and pore diameter of catalysts were determined by nitrogen gas adsorption at liquid nitrogen temperature (-196°C) using Micromeritics ChemiSorb 2750 Pulse chemisorption System instrument. Before characterization, the sample was thermally treated at 150°C for 1h.

3.2.3 Temperature programmed adsorption (NH_3-TPD)

The acid properties of catalysts were investigated by temperature programmed adsorption of ammonia (NH_3-TPD) equipment by using Micromeritics chemisorp 2750 Pulse Chemisorption System. In an experiment, a packed quartz wool and 0.1g of catalyst was loaded in a quartz tube and pretreated at 500°C under helium flow. The sample was saturated with 15%NH_3/He. After saturation, the physisorbed ammonia was desorbed under helium gas flow about 30 min. and then the sample was heated from 40°C to 800°C at heating rate 10°C/min. The amount of ammonia in effluent was measured via TCD signal as a function of temperature.

3.2.4 Scanning electron microscopy (SEM)

Scanning electron microscopy was employed the determination of the shape and size of the prepared catalyst. The JEOL JSM-35 CF model at the Scientific and Technological Research Equipment Center, Chulalongkorn University (STREC) is used for this purpose.

3.2.5 Transmission electron microscopy (TEM)

The morphology and crystallite size of all catalysts were observed by using JEOL-JEM 20°CX transmission electron microscope operated at 100 kV at National Metal and Materials Technology Center. The average crystallite size was measured by SemAfore program version 5.00.

3.3 Reaction study in dehydration of ethanol

In this proposed research, the ethanol dehydration reaction was tested in gas phase at atmospheric pressure. The reaction is investigated for all catalysts using the apparatus as shown in **Figure 3.1**

3.3.1 Chemicals and reagents

Table 3.2 displays the chemicals and the reagents used in the ethanol dehydration reaction.

Table 3.2 The chemicals and reagents were used in the reaction.

Chemicals and Reagents	Supplier
High purity grade hydrogen (99.99%)	TIG
Ultra high purity nitrogen gas (99.99%)	TIG
Argon	TIG
Ethanol	Merck

3.3.2 Instruments and apparatus

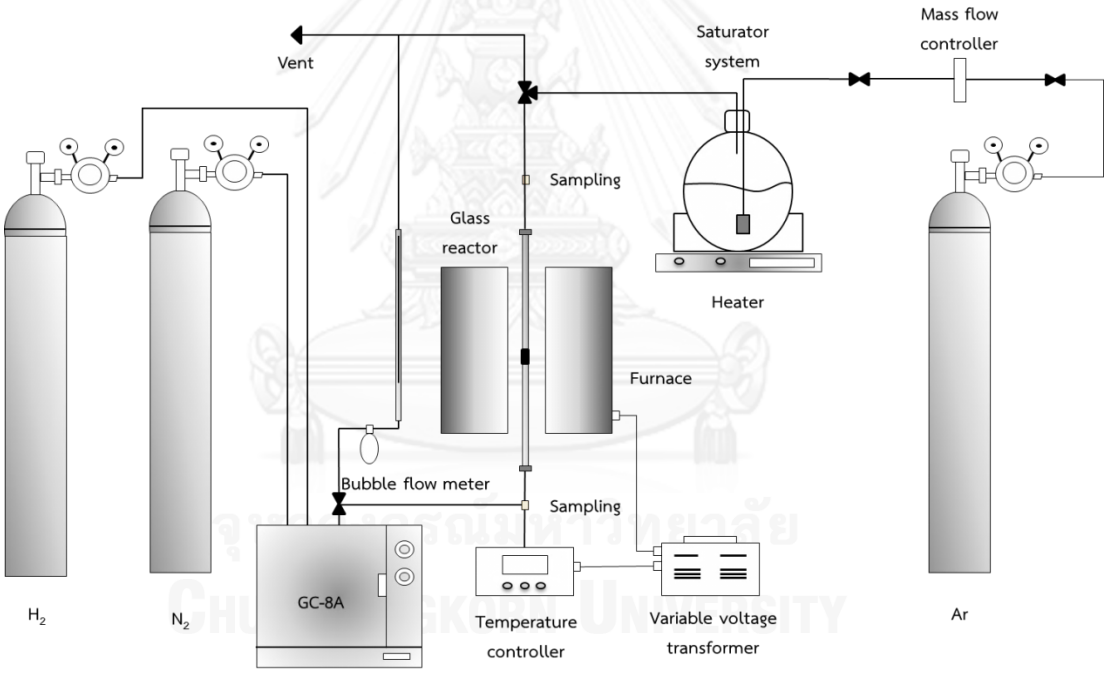

Figure 3.1 Ethanol dehydration system.

Figure 3.1 shows the system of the ethanol dehydration which all equipment using for catalytic tests consist of:

(a) Reactor: The reactor tube is made from glass tube (borosilicate type) with an inner diameter 0.7mm.

(b) Saturator: The saturator is made from glass. The role of the saturator is to produce ethanol saturated vapor from liquid ethanol which is set to bubble ethanol by feeding argon gas and providing heat by a hot-plate. The saturator is operating at atmospheric pressure.

(c) Furnace and heating cable: The furnace is provided heat for the reactor. The temperature of the furnace is controlled by interoperability of variable voltage transformer and temperature controller. For heating cable, it is warped with the line at outlet of reactor. The heating cable is used to prevent the condensation of water dehydrated from reaction.

(d) Temperature controller: The temperature of furnace is established a set point at any temperatures in range between 200℃ to 400℃ by temperature controller which is connected to thermocouple attached to the reactor and a variable voltage transformer.

(e) Gas controlling system: Argon is used to carrier ethanol vapor into the system. It is set with a pressure regulator, an on-off valve and mass flow controller are used to adjust the flow rate of carrier gas.

(f) Gas chromatography (GC): A Gas chromatography equipped (Shimadzu GC-14A) with flame ionization detector (FID) with DB-5 capillary column, which is used to analyze the feed and product. The operating condition for gas chromatography is reported;

- Detector: FID
- Capillary column**:** DB-5
- Carrier gas**:**Nitrogen (99.99vol.%) and Hydrogen (99.99vol.%)
- Column temperature

- Initial: 40 °C
- Final: 40 °C

- Injector temperature: 150 °C
- Detector temperature: 150 °C
- Time analysis: 12min

3.2.3 Ethanol dehydration reaction procedure

The dehydration of ethanol was carried out in a fixed-bed continuous flow reactor with an inner diameter 0.7mm. In the experiment, 0.01g of a packed quartz wool and about 0.05g of catalyst was loaded into the reactor, and then the catalyst was pretreated in argon (50ml/min) at 200°C for 1h under atmospheric pressure. The reaction was carried out in temperature ranging from 200°C to 400°C. The products were analyzed by a Shimadzu GC8A gas chromatograph with FID using capillaly column (DB-5) at 150°C.

CHAPTER IV

RESULTS AND DISCUSSION

Chapter IV describes the results and discussion on the effect of calcination temperature and metal oxide loading on the mixed γ- and χ-crystalline phase alumina. The characteristic of all catalyst was investigated by X-ray diffraction (XRD), nitrogen physisorption, scanning electron microscopy (SEM), and temperature programmed adsorption (NH_3-TPD). Moreover, all catalysts were tested in ethanol dehydration reaction, considered the suitable catalysts and conditions for ethanol dehydration.

In this chapter, it is divided into 2 parts. For section 4.1, the effect of calcination temperature on mixed γ- and χ-crystalline-phase alumina catalysts for ethanol dehydration was studied. Later, the effect of MoO_3 loading over mixed γ- and χ-crystalline phase alumina catalyst for ethanol dehydration was discussed in section 4.2.

4.1 Effect of calcination temperature on mixed gamma- and chi-crystalline-phase alumina catalysts for ethanol dehydration.

4.1.1 Catalyst characterization

4.1.1.1 X-ray diffraction (XRD)

X-ray diffraction technique was used to identify the structure of catalysts. **Figure 4.1** shows XRD patterns of mixed-phase alumina catalysts prepared by the solvothermal method of the mixed solution between toluene and 1-butanol.

The catalysts were calcined with various temperatures in the range of 400°C to 1000°C. It was found that the XRD patterns of catalysts C50-400, C50-500, C50-600, C50-700, and C50-800 calcined at 400°C to 800°C, were similar. These patterns indicated the presence of γ- crystalline (32°, 37°, 39°, 45°, 61° and 66°) and χ-crystalline (37°, 40°, 43°, 46°, 60° and 67°) phases of alumina [10]. However, the C50-1000 catalyst calcined above 900°C exhibits the different XRD pattern probably due to the transformation to delta and theta phases [40]. The obtained catalysts remained mixed γ- and χ-crystalline phase, even they were calcined in the range of 400°C to 900°C.

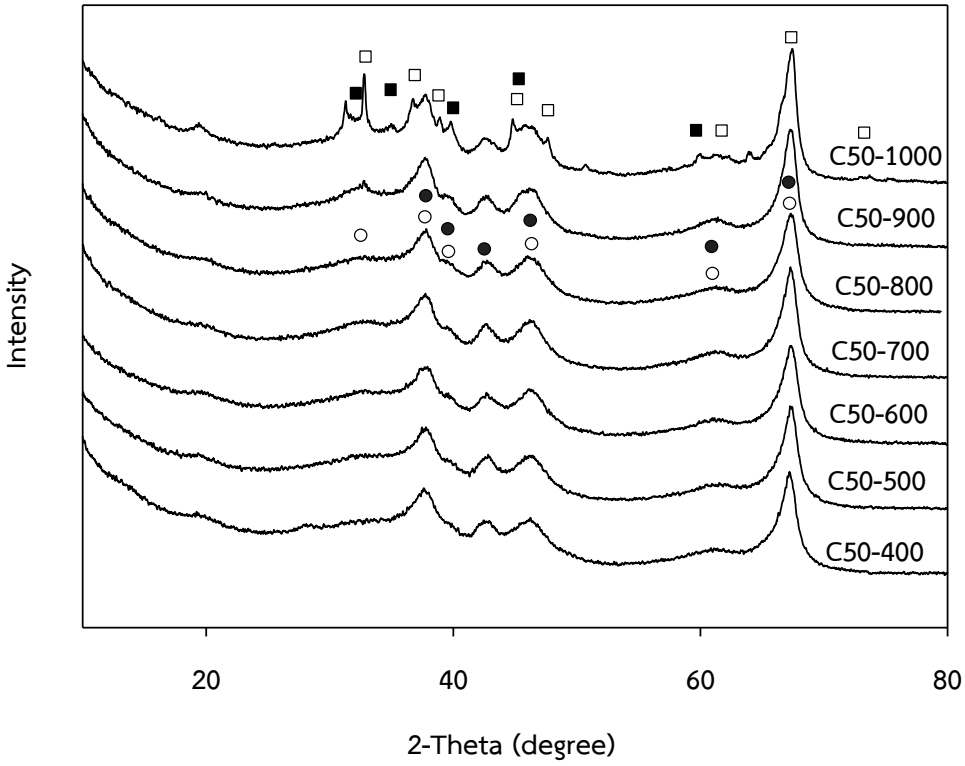

Figure 4.1 XRD patterns of mixed γ- and χ-crystalline phase alumina catalysts with various calcination temperatures; (○) gamma-alumina, (●) chi-alumina, (□) theta-alumina and (■) delta-alumina.

4.1.1.2 Nitrogen physisorption

BET surface area, pore volume, and pore size diameter of catalysts with various calcination temperature are summarized in **Table 4.1.** The BET surface area slightly decreased with an increasing calcination temperature. Surface area decreased from 233 to 144m^2/g with calcination temperature from 400°C to 1000°C. The pore volume was found to be in the order: C50-600 > C50-500 > C50-400 > C50-700 ≈ C50-800 > C50-900 > C50-1000. The pore volume of alumina catalysts seems to be constant with an increase in the calcination temperature. The C50-600 shows the highest pore volume (0.57m^3/g). All catalysts exhibited increased pore size diameter from 5.94 to 9.14nm with increasing calcination temperature. **Figure 4.2** shows the N_2 adsorption–desorption isotherms of the C50-400, C50-600, C50-800, and C50-1000 catalysts. According to the IUPAC classification of physisorption isotherms, the isotherms of all catalysts apparently correspond to type IV isotherms. It means that all catalysts displays mesoporous structure and contain pore with diameter between 2 and 50nm. The different calcination temperature did not affect the pore structure of catalyst.

Table 4.1 BET surface area, pore volume, and pore size diameter of the mixed γ- and χ-crystalline phase alumina catalysts.

Sample	BET surface area S_{BET} (m^2/g)	Pore volume P_V (m^3/g)	Pore size diameter P_d (nm)
C50-400	233	0.53	5.94
C50-500	191	0.54	7.29
C50-600	187	0.57	8.09
C50-700	157	0.51	8.39
C50-800	149	0.51	8.51
C50-900	142	0.49	8.98
C50-1000	114	0.42	9.41

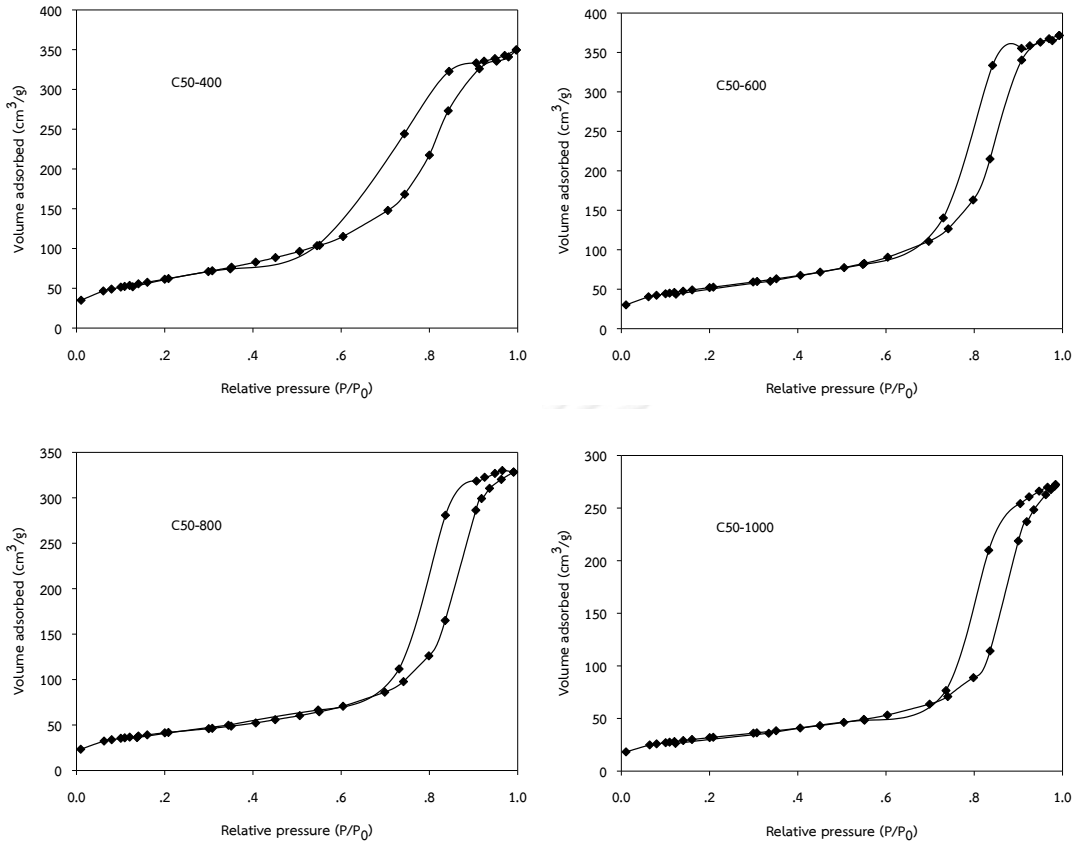

Figure 4.2 The N_2 adsorption–desorption isotherms of mixed γ- and χ-crystalline phase alumina catalysts with various calcination temperatures.

The variation in pore size distribution with the different calcination temperatures of catalysts are shown in **Figure 4.3.** All catalysts have a unimodal pore size distribution and the pore size is attributed in the range of 2.86 to 14.99nm. When calcination temperature increased, the C50-400 exhibited the average pore sizes diameter around 9.49nm and pore volume about 0.53m^3/g, whereas the C50-1000 showed the average pore sizes diameter and pore volume about 14.54nm and 0.42m^3/g, respectively. It is suggested that an increase in calcination temperature aggregated the catalyst resulting in losing the surface area, increasing the pore sizes diameter, and decreasing the pore volume.

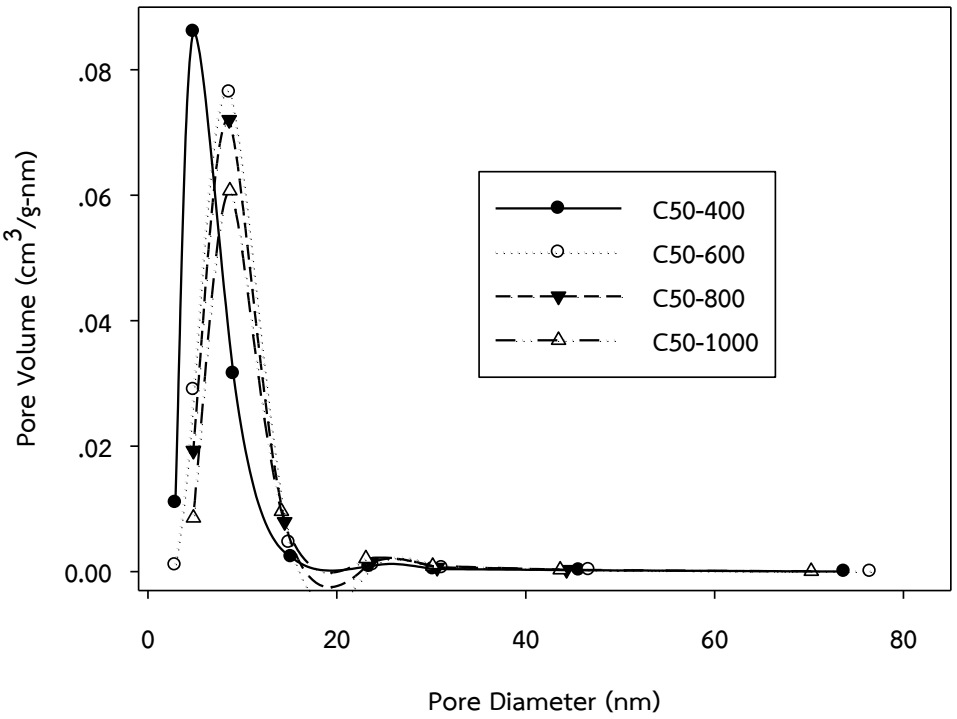

Figure 4.3 Pore size distribution of mixed γ- and χ-crystalline phase alumina catalysts with various calcination temperatures.

4.1.1.3 Scanning electron microscopy (SEM)

Morphologies of mixed phase alumina catalysts with various calcination temperatures observed by SEM technique are shown in **Figure 4.4.** It was found that the calcination temperature did not affect the catalyst morphologies. All catalysts show similar morphological features

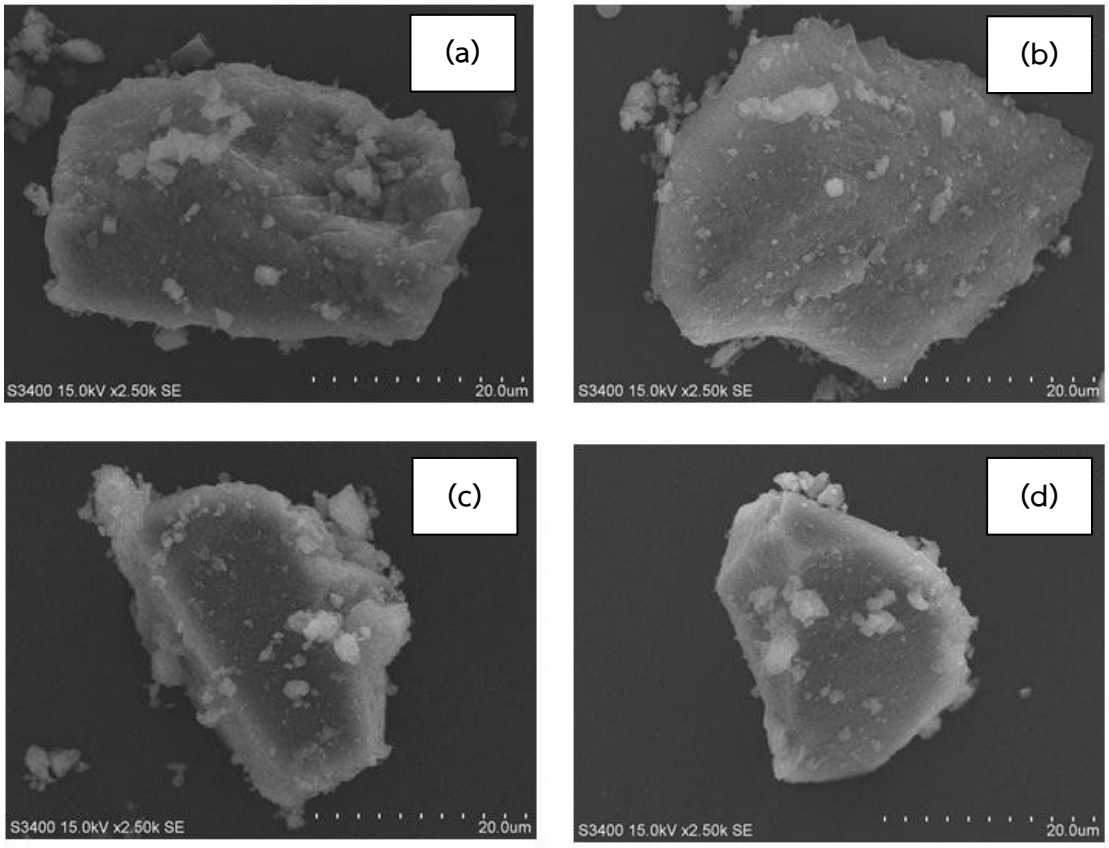

Figure 4.4 SEM micrograph of mixed γ- and χ-crystalline phase alumina catalysts with various calcination temperatures: (a) C50-400, (b) C50-600, (c) C50-800 and (d) C50-1000.

4.1.1.4 Transmission electron microscopy (TEM)

From the previous section, it was suggested that an increase of calcination temperature insignificantly affects on the morphologies of mixed γ- and χ-crystalline phase alumina catalysts. However, Pansanga et al. [12] reported the morphology of mixed phase alumina which was obtained by transmission electron microscopy technique (TEM). They found that the morphology of alumina with different phases was presented different structure. The morphologies of mixed γ- and χ-crystalline-phase alumina exhibited wrinkled sheets and spherical particles of γ- and χ-crystalline phase alumina, respectively.

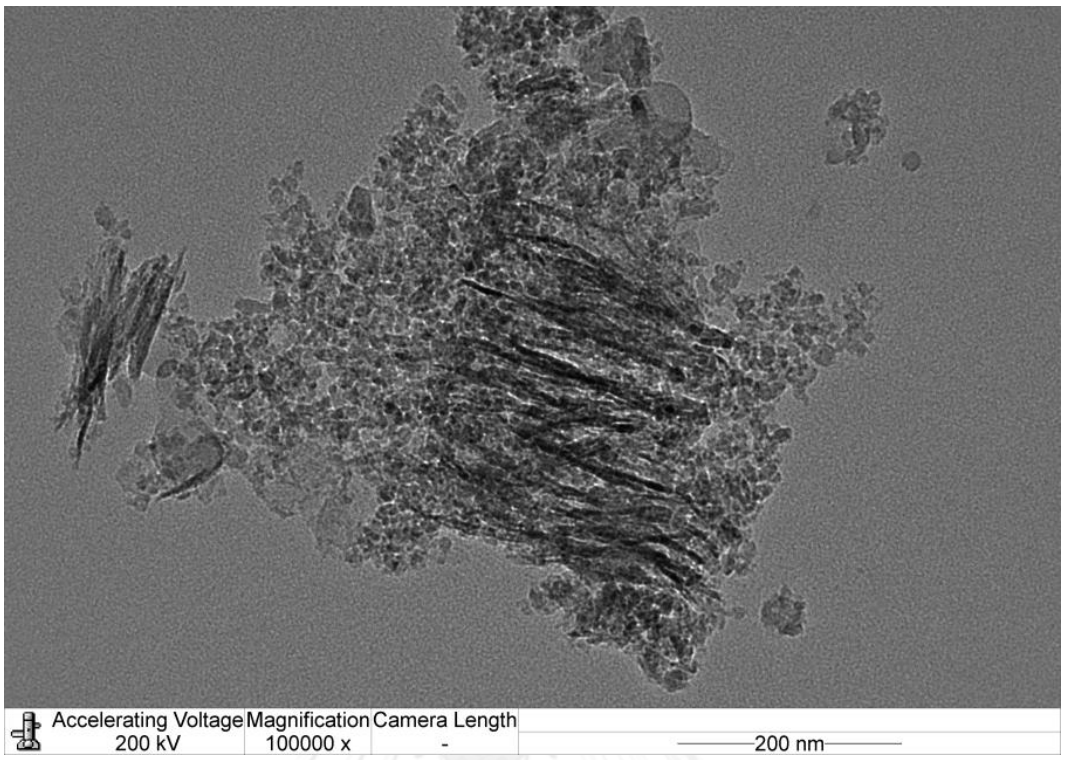

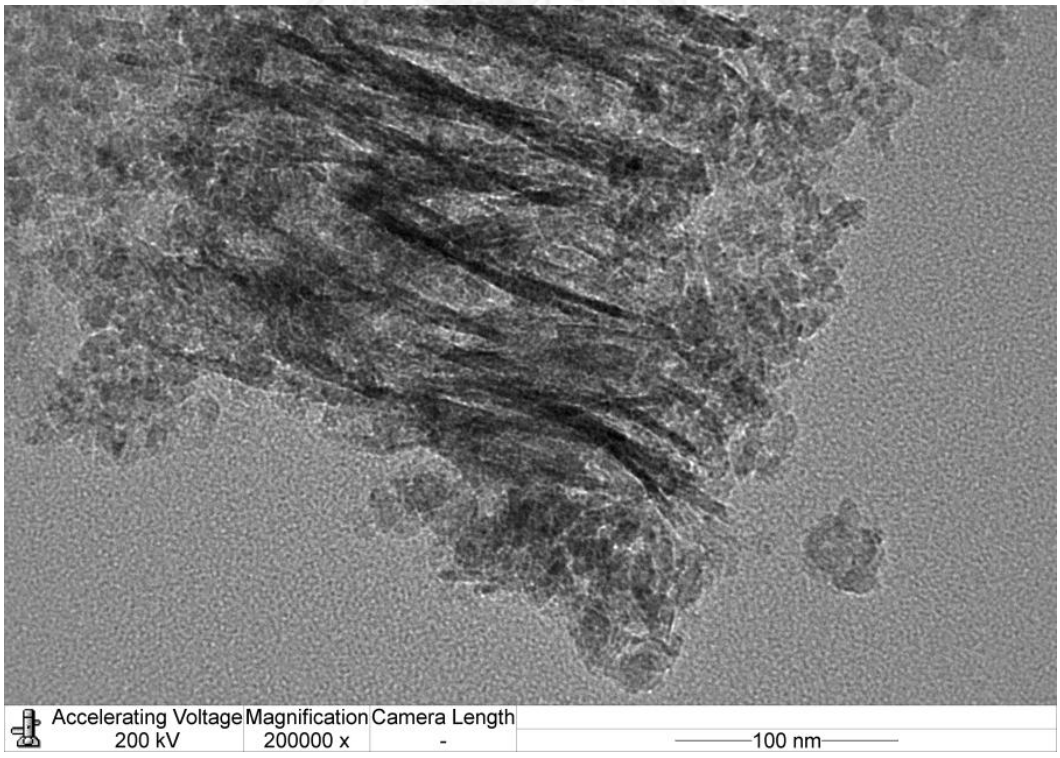

Figure 4.5 TEM micrograph of the C50-400.

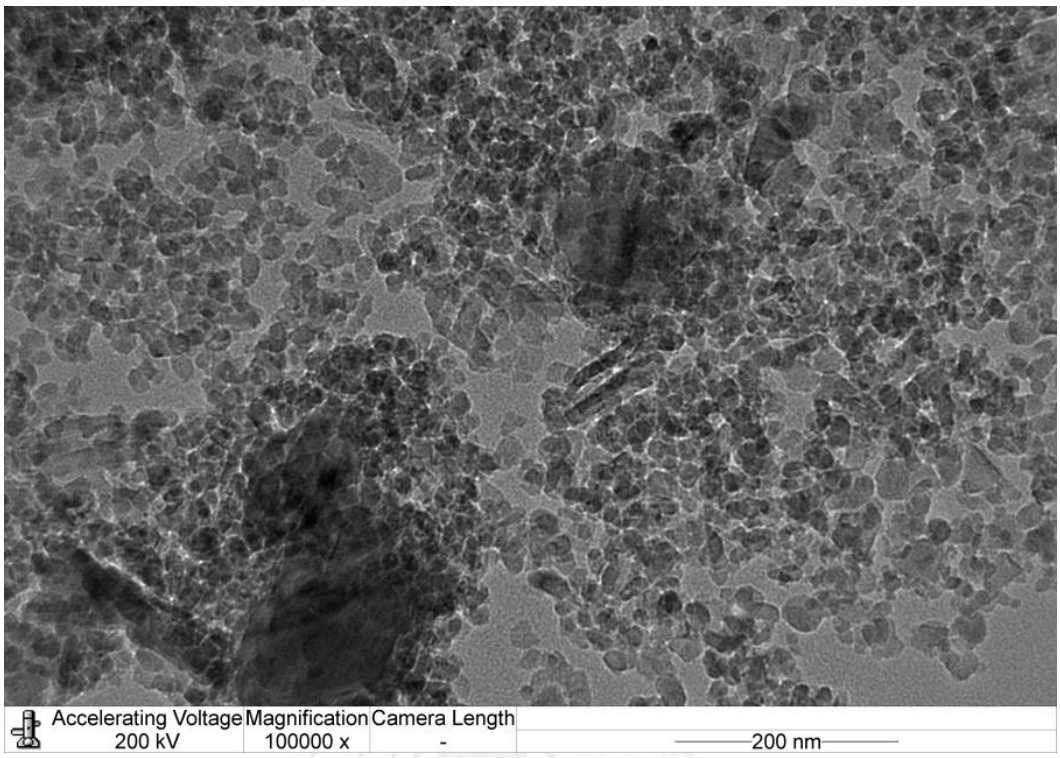

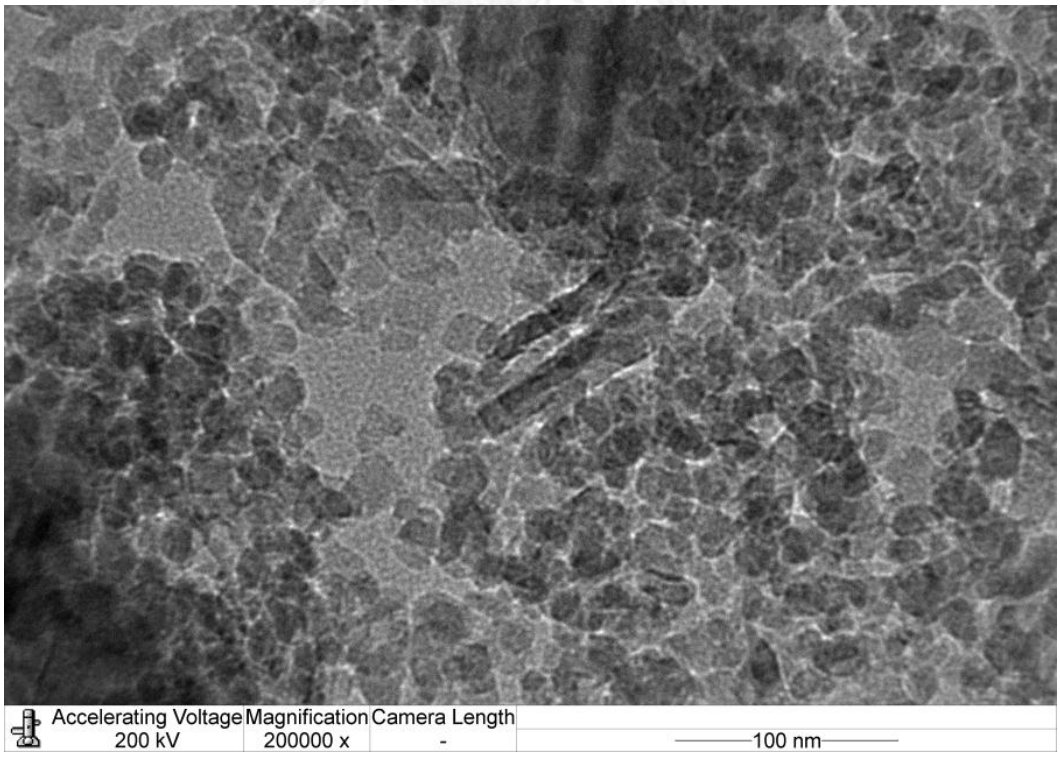

Figure 4.6 TEM micrograph of the C50-1000.

Figure 4.5 and **4.6** show the TEM micrographs of the C50-400 and C50-1000, it confirm in the obtained catalysts contain the mixed γ- and χ-crystalline-phase alumina because it consists of wrinkled sheets and spherical particles, according to Pansanga et al. [12]. Although, the calcination temperature insignificantly affects on the morphologies investigated by SEM, it significantly affects on the phases investigated by XRD. The TEM can be confirmed in this result. **Figure 4.5** shows two types of morphologies, which is mixed phase γ- and χ- alumina calcined at 400°C. Whereas the calcination temperature increased about 1000°C, the XRD suggested that the structure was transformed to other phases. It was proven by TEM as seen in **Figure 4.6** that it almost appears as spherical particles and scarcely occur wrinkled sheets. It is suggested that the wrinkled sheets (γ- phase alumina) transformed to other phase while the spherical particles (χ- phase alumina) remain unchanged. It is in good agreement with the XRD technique as seen for the peaks of C50-1000 at 43°. This indicated that χ- phase alumina was still outstanding. On the other hand, the peaks of γ- phase alumina were observed differently.

4.1.1.5 Temperature programmed adsorption (NH_3-TPD)

The NH_3-TPD profiles of mixed phase alumina catalysts with various calcination temperatures are shown in **Figure 4.7.** It can be seen that TPD profile of each catalyst exhibited only one broad peak at the temperature range around 100 to 500°C. According to Khom-in et al. [10], they reported that the broad peak consisted of two peaks which were in the range of 100 to 230°C and 250 to 500°C, respectively. Generally, the peak at lower temperature was attributed to weak acid sites, whereas the higher temperature was associated with medium to strong acid sites. As can be seen in **Figure 4.7**, both peaks were decreased with an increase in the calcination temperature. These results are corresponded in a decrease total surface acidity of catalyst from 705 to 337μmol/g cat. as shown in **Table 4.2**.

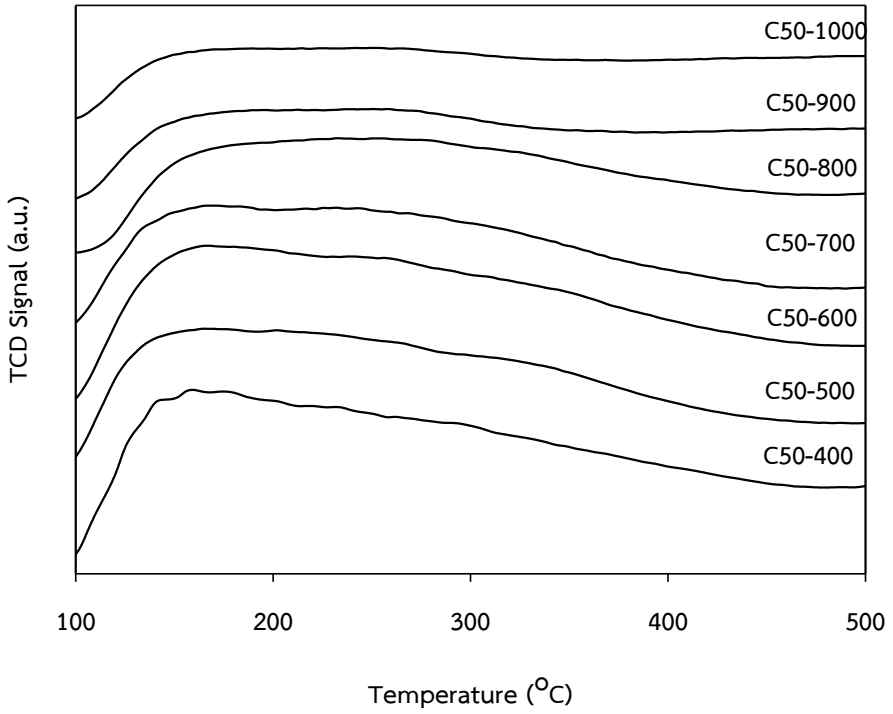

Figure 4.7 NH_3-TPD profiles of mixed γ- and χ-crystalline phase alumina catalysts with various calcination temperatures.

Table 4.2 summarizes the amount of acidity over different catalysts. It was found that the total acidity was significantly decreased with increasing the calcination temperature. This is due to the hydroxyl group on catalyst surface was released with increasing the calcination temperature, leading to lower acidity. Besides, the total acidity can be divided into two types of acidic sites; a weak acid sites and medium to strong acid sites. For weak acid sites, the position of weak acid sites exhibited the amount of NH_3 desorption in the range from 215 to 109μmol NH_3/g cat. The C50-400 exhibited the highest acidity. However, the position of medium to strong acid sites presented in the range from 705 to 337μmol NH_3/g cat. The medium to strong acidity of catalyst was in the order: C50-600 > C50-500 > C50-400 > C50-700 > C50-800 > C50-900 > C50-1000.

Table 4.2 The amount of acidity of mixed γ- and χ-crystalline-phase alumina catalysts with various calcination temperatures.

Sample	NH_3 desorption (μmol NH_3/g cat.)		Total acidity (μmol NH_3/g cat.)
	Weak	Medium to strong	
C50-400	215	489	705
C50-500	195	494	689
C50-600	148	513	661
C50-700	155	387	542
C50-800	109	364	473
C50-900	172	230	402
C50-1000	146	191	337

4.1.2 Catalytic activity

The catalytic performance of the mixed phase alumina catalysts was tested in ethanol dehydration. First, 0.05g of catalyst was added into the fixed-bed reactor, then gas phase ethanol having flow rate of 50ml/min was flowed into the reactor. The reaction was carried out in the temperature ranging from 200°C to 400°C.

The catalytic activity depends on the operating temperature, according to previous reports [6-8]. The results of catalytic activity were reported in terms of conversion and selectivity versus temperature profile. Besides the operating temperature, the catalyst acidity property is an important factor influencing on the conversion and selectivity of ethanol. Ferreira et al. [32] studied the dehydration of ethanol over acid catalyst and found that the products of ethanol dehydration reaction are ethylene (main product), DEE and acetaldehyde. The ethylene formation is favored by medium to stronger acid sites, whereas DEE requires only weak acid sites. At low temperature, DEE is the major product, while at high temperature, ethylene is majority.

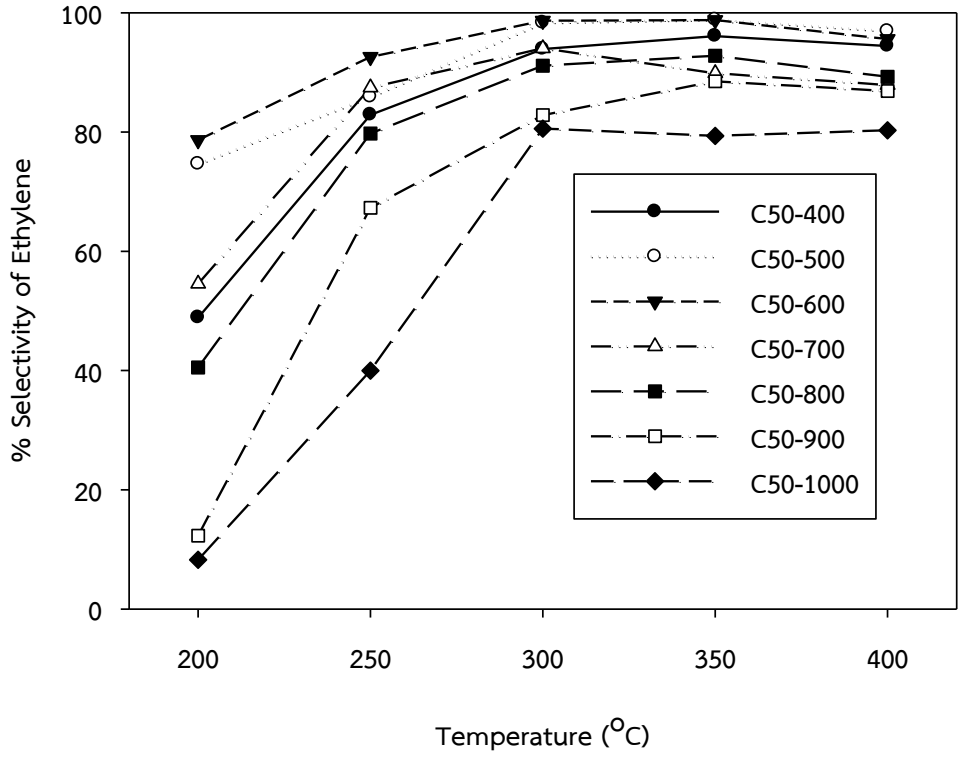

Figure 4.8 Selectivity of ethylene profiles in ethanol dehydration at different temperatures.

Figures 4.8 to **4.10** show the selectivity of ethylene, DEE and acetaldehyde, respectively. At high temperature, the selective of ethylene for all catalysts was higher than that at low temperature as shown in **Figure 4.8.** On the contrary, the selectivity of DEE apparently decreased with increasing temperature as seen in **Figure 4.9.** This result can be ascribed by thermodynamic properties, the reaction of ethanol to ethylene is endothermic reaction. Thus it requires high temperature. On the other hand, the reaction of ethanol to DEE is exothermic reaction, therefore DEE is favor at the lower temperature. For the selectivity of acetaldehyde, it is presented in **Figure 4.10.** It can be observed the relatively constant under 10% selectivity for all catalysts excepting for the C50-900 and C50-1000. This may be attributed to the phase transformation of catalysts according to

XRD patterns as shown in **Figure 4.1.** It would be appropriate to promote acetaldehyde.

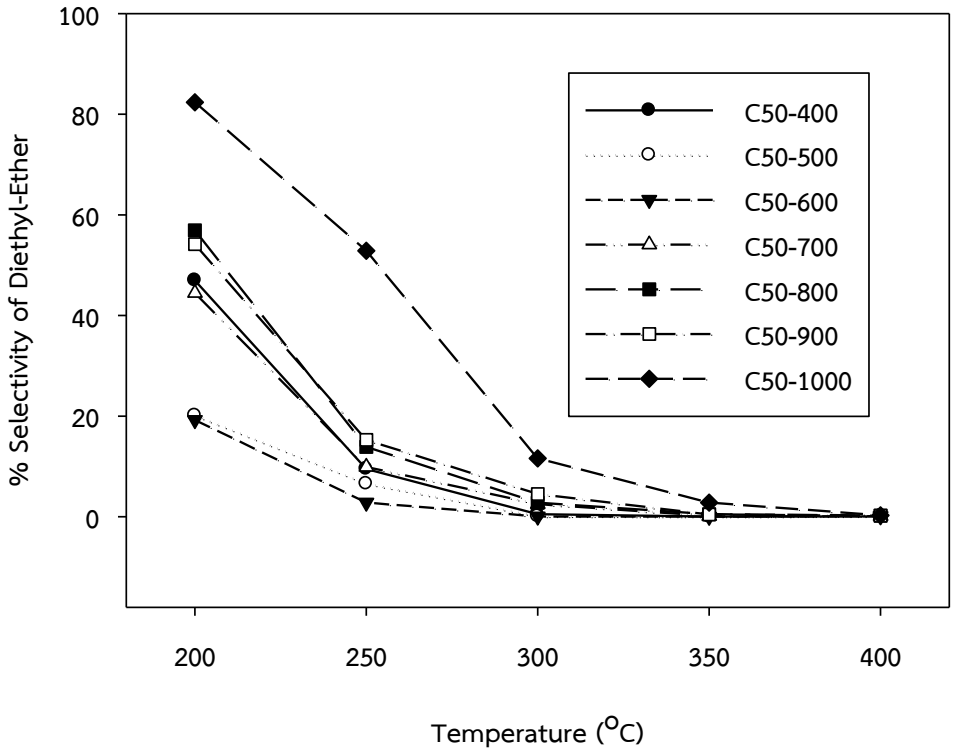

Figure 4.9 Selectivity of DEE profiles in ethanol dehydration at different temperatures.

The acidity results are summarized in **Table 4.2**. The C50-600 exhibited the highest medium to strong acidity, followed by the C50-500 and C50-400. The order of ethylene selectivity shows the same ethanol conversion. This result is in agreement with pervious report [32]. For the C50-1000, it exhibited the lowest medium to strong acidity. Thus, the ethylene selectivity of C50-1000 was lower than other catalysts. In terms of the DEE selectivity, it was in order of C50-1000 > C50-900 > C50-800 > C50-700 > C50-400 > C50-500 > C50-600. This result showed the opposite trend compared to the selectivity of ethylene. It was due to the ethanol to DEE requires weak acid sites as mentioned above.

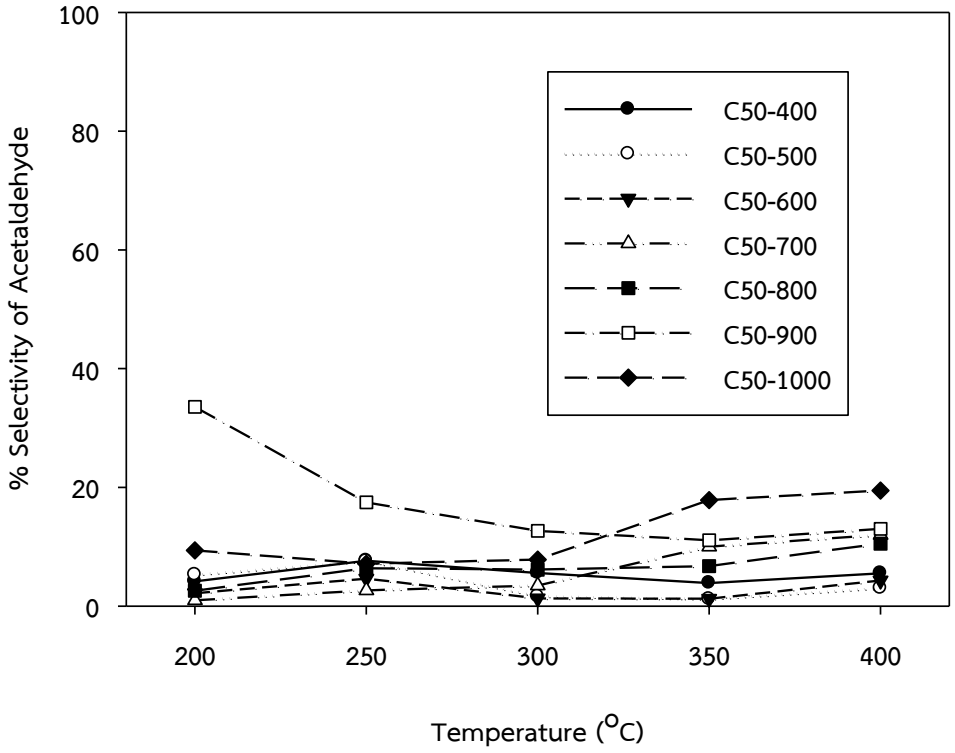

Figure 4.10 Selectivity of acetaldehyde profiles in ethanol dehydration at different temperatures.

Figure 4.11 shows the ethanol conversion in the range of 200°C to 400°C. The ethanol conversion was in order of C50-600 > C50-500 > C50-400 > C50-700 > C50-800 > C50-900 > C50-1000. Similar trend was observed for all catalysts. The ethanol conversion increased with an increase in reaction temperature. The C50-400, C50-500 and C50-600 catalysts showed good performance with 100% ethanol conversion. However, at temperature higher than 400°C, deactivation can occur and products can be converted to other products [40]. Considering the relationship between acidity and ethanol conversion, it was found that the medium to strong acidity plays an important role in the ethanol conversion.

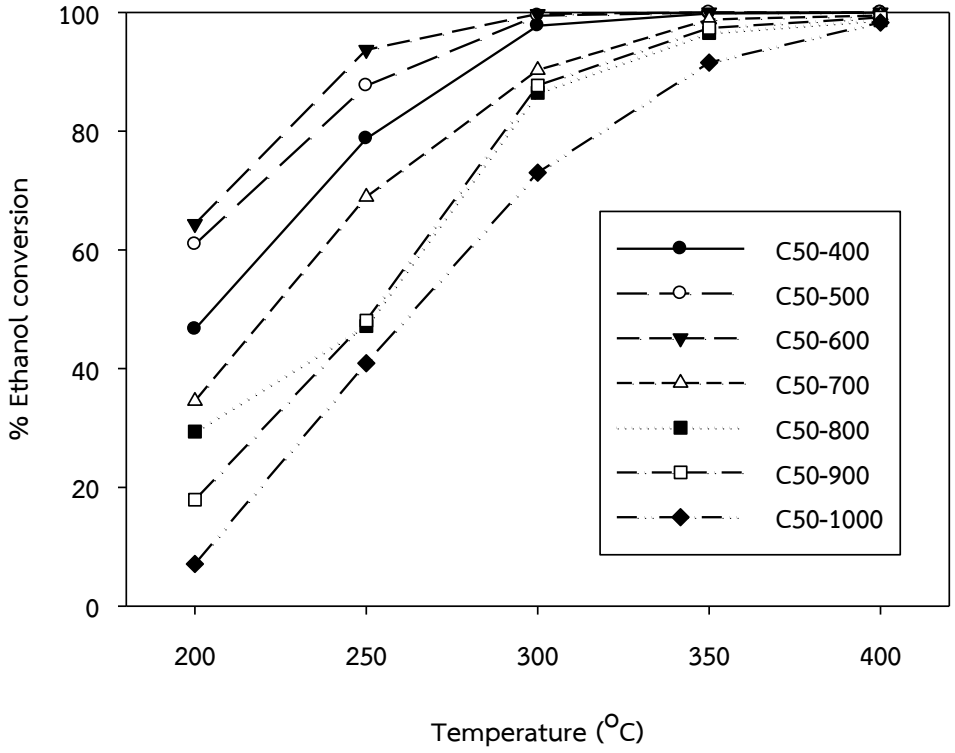

Figure 4.11 Ethanol conversion profiles in ethanol dehydration at different temperatures.

In this section, the mixed γ- and χ-crystalline-phase alumina catalysts were investigated upon the effect of calcination temperatures. The results revealed that the acidity decreased significantly with increased calcination temperature. The C50-400, which was calcined at 400°C displays the highest acidity while the C50-1000, calcined at 1000°C exhibited the lowest acidity. All catalysts were measured upon the catalytic performance in ethanol dehydration reaction under atmospheric pressure and temperature between 200°C to 400°C. It reveals that the C50-600 shows the highest for both ethanol conversion and ethylene selectivity. Although, the acidity of the C50-600 has a value of the third rank, the catalytic performance is the highest. This is due to the effect of medium to strong acid sites. It is known that the medium to strong acid sites of catalysts plays an important role on the catalytic activity for ethanol dehydration.

4.2 Effect of MoO_3 loading over mixed gamma- and chi- crystalline phase alumina catalyst for ethanol dehydration.

From section 4.1, the mixed γ- and χ-crystalline phase alumina catalysts calcined at 600°C (C50-600) exhibited the highest the catalytic performance. Therefore, the C50-600 was selected as the catalyst to study the characteristic and catalytic performance with the modification of MoO_3 for ethanol dehydration reaction.

4.2.1 Catalyst characterization

4.2.1.1 X-ray diffraction (XRD)

X-ray diffraction patterns of MoO_3-modified catalyst are shown in **Figure 4.12**. XRD patterns were used as referentce to compare the mixed phase alumina and MoO_3. For MoO_3-modified alumina, the catalysts were prepared by impregnation method using ammonium heptamolybdate-tetrahydat $[(NH_4)_5Mo_7O_{34}\bullet 4H_2O]$ as a precursor and calcined at 500°C. It can be seen for 5Mo/C50-600 and 10Mo/C50-600 that no distinguishable peak was observed in XRD patterns and this peak was found only for the mixed γ- and χ-crystalline-phase alumina. It means that, at low MoO_3 loading (10wt.%), MoO_3 was well dispersed on alumina surface. On the contrary, the sample with high amount of MoO_3 (15wt.% - 20 wt.%), showed peaks at 2θ of 27.3°, 25.7°, and 23.3°, which are characteristics of MoO_3 [41]. The intensity of the diffraction peak can be ascribed to an increase of MoO_3 indicating the formation of crystalline MoO_3 on alumina surface.

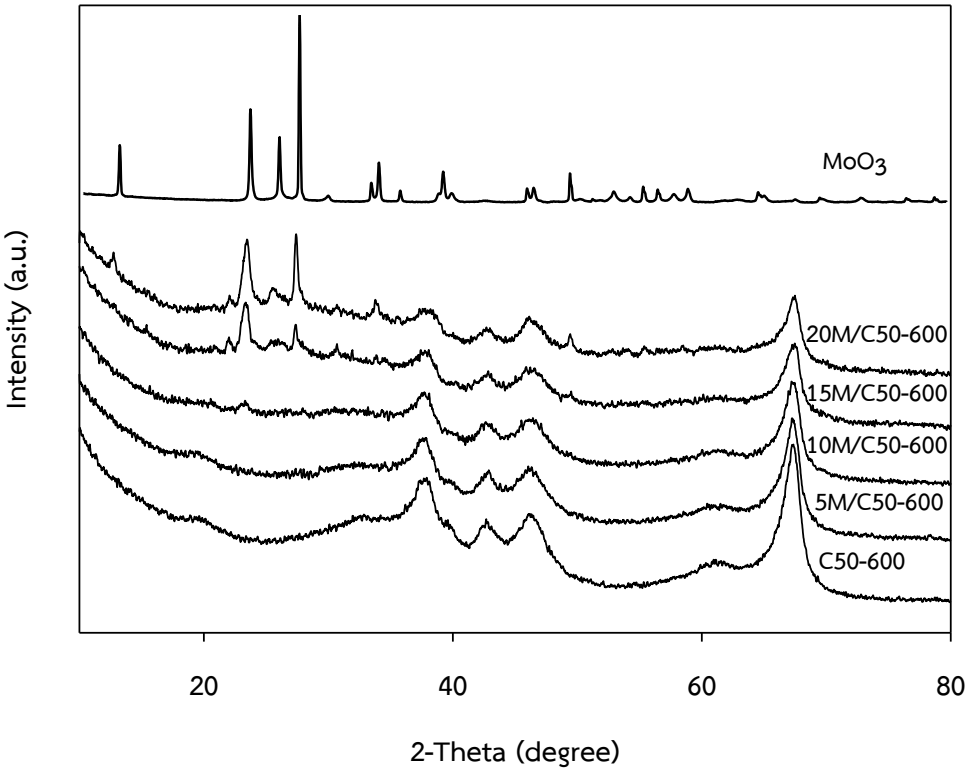

Figure 4.12 XRD patterns of mixed γ- and χ-crystalline phase alumina, MoO_3-modified alumina, and MoO_3.

4.2.1.2 Nitrogen physisorption

Table 4.3 summarizes the BET surface area (S_{BET}), pore volume (P_v), and pore size diameter (P_d) of all catalysts. It can be seen that the S_{BET}, P_v, and P_d of modified catalysts was decreased compared to the unmodified catalyst (C50-600). The S_{BET} and P_v were decreased with an increase of MoO_3 loading. This may be due to the accumulation of the MoO_3 on alumina surface. Although the 5Mo/C50-600 and 10Mo/C50-600 did not reveal the MoO_3 species, the S_{BET}, P_v, and P_d of both catalyst were decreased. This indicated that MoO_3 was well dispersed on the support surface probably as the monolayer according to [42]. However, at higher MoO_3 loading (20Mo/C50-600), it is clearly seen the decrease of the S_{BET} and P_v because the formation of MoO_3 crystallization obstructs the small pores and/or surface of

catalysts. Moreover, with MoO_3 loading more than 16wt.%, it results in decreased S_{BET} and P_v, the Mo species dispersed on the surface of support as monolayer is 4.04 Mo atoms/nm^2, approximately 16wt.%. Also, the 20Mo/C50-600 implied that the dispersion of MoO_3 on surface was not monolayer, it brought about to lose surface area. For pore size diameter, it was found to be in the order: 10Mo/C50-600 > 15Mo/C50-400 > 5Mo/C50-800 > 20Mo/C50-1000, which was in the range of 7.20 to 6.74nm. The pore size diameter of modified catalyst was lower than C50-600 almost twice. This is result due to the covering of MoO_3 on surface and pore of catalysts. **Figure 4.13** shows the N_2 adsorption–desorption isotherms of the modified MoO_3 mixed phase catalysts. The isotherms of all catalysts are corresponded to type IV isotherms, indicating the characteristic of mesoporous structure. Although the catalyst was modified with different amount of MoO_3, the isotherm was similar. In addition, the volume of nitrogen adsorbed decreased with increasing MoO_3. Therefore, the feature of the pore catalysts was unaffected by MoO_3 loading.

Table 4.3 BET surface area, pore volume, and pore size diameter of the MoO_3 over mixed γ- and χ-crystalline phase alumina catalysts with various MoO_3 loading.

Sample	BET surface area	Pore volume	Pore size diameter
	S_{BET} (m^2/g)	P_v (m^3/g)	P_d (nm)
C50-600	187	0.57	8.09
5Mo/C50-600	185	0.45	6.88
10Mo/C50-600	164	0.43	7.20
15Mo/C50-600	134	0.35	7.12
20Mo/C50-600	131	0.35	6.74

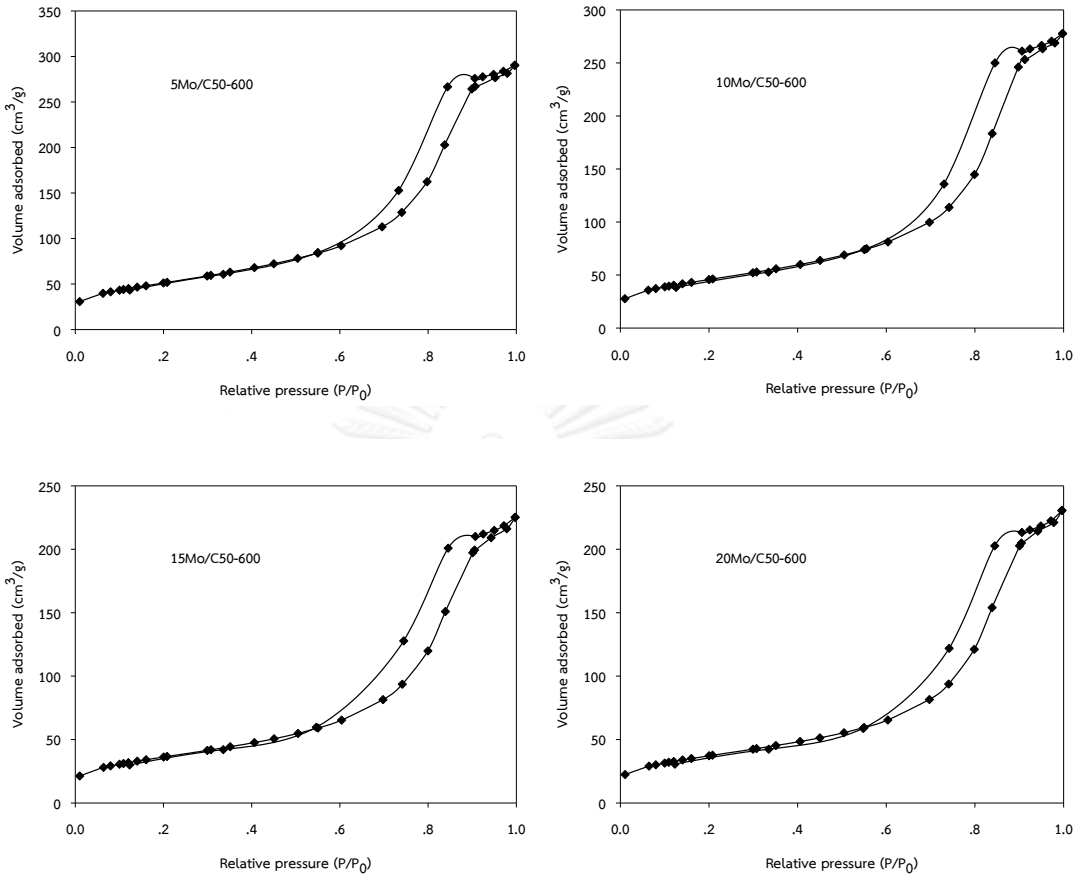

Figure 4.13 The N_2 adsorption–desorption isotherms of the MoO_3 over mixed γ- and χ-crystalline phase alumina catalysts with various MoO_3 loading.

In term of pore size distribution, all catalysts were attributed in the range of 1.71 to 15.18nm. This indicated the mesoporous structure. The pore size distribution was apparent a unimodal as shown in **Figure 4.14.** In addition, it was found that the increasing of MoO_3 loading from 5 to 20wt.% resulted in a decrease in the pore volume from 0.452 to 0.350m^3/g, respectively. Thus, this result suggests that MoO_3 loading rarely affects on pore sizes distribution.

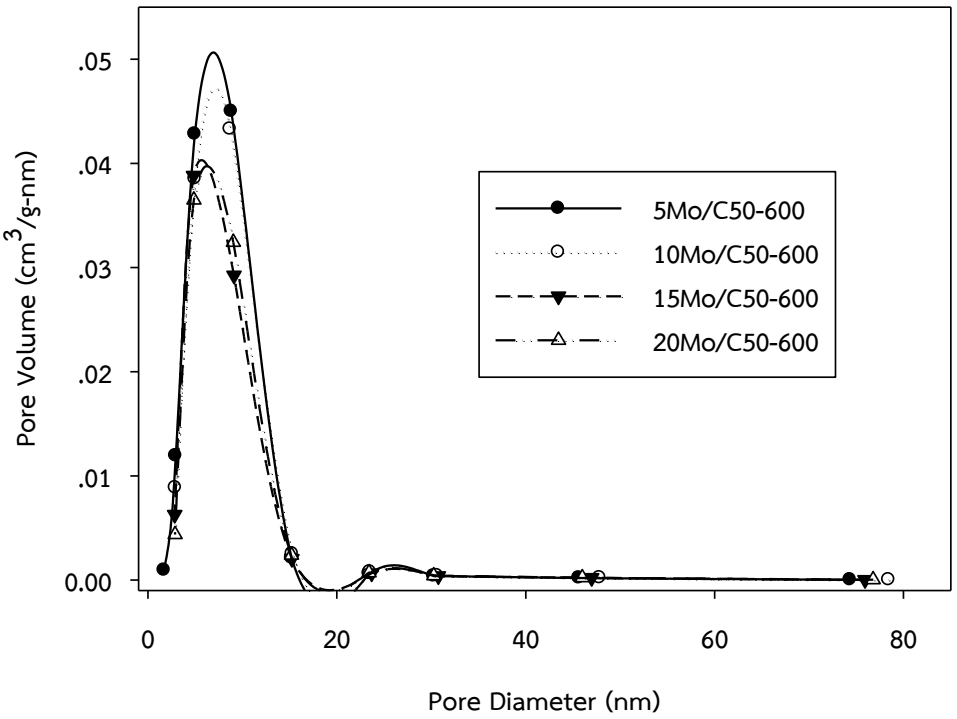

Figure 4.14 Pore size distribution of the MoO_3 over mixed γ- and χ-crystalline phase alumina catalysts with various MoO_3 loading.

4.2.1.3 Scanning electron microscopy (SEM)

The morphologies of the MoO_3 over different catalysts examined by Scanning Electron Microscopy (SEM) are shown in **Figure 4.15.** The modified catalyst had the spherical particle while the fine particle was found for unmodified catalyst. This is probably due to the MoO_3 aggregation. In addition, SEM images of each particle exhibited the MoO_3 accumulation on surface catalysts, which was in good agreement with the XRD result in **Figure 4.12.**The 5Mo/C50-600 did not reveal the XRD peak of MoO_3, which is due to well dispersion, whereas the 20Mo/C50-600 shows MoO_3 peak, indicating the formation of crystalline MoO_3 on alumina surface. It can be concluded that the increase of MoO_3 leads to the crystalline MoO_3 formation.

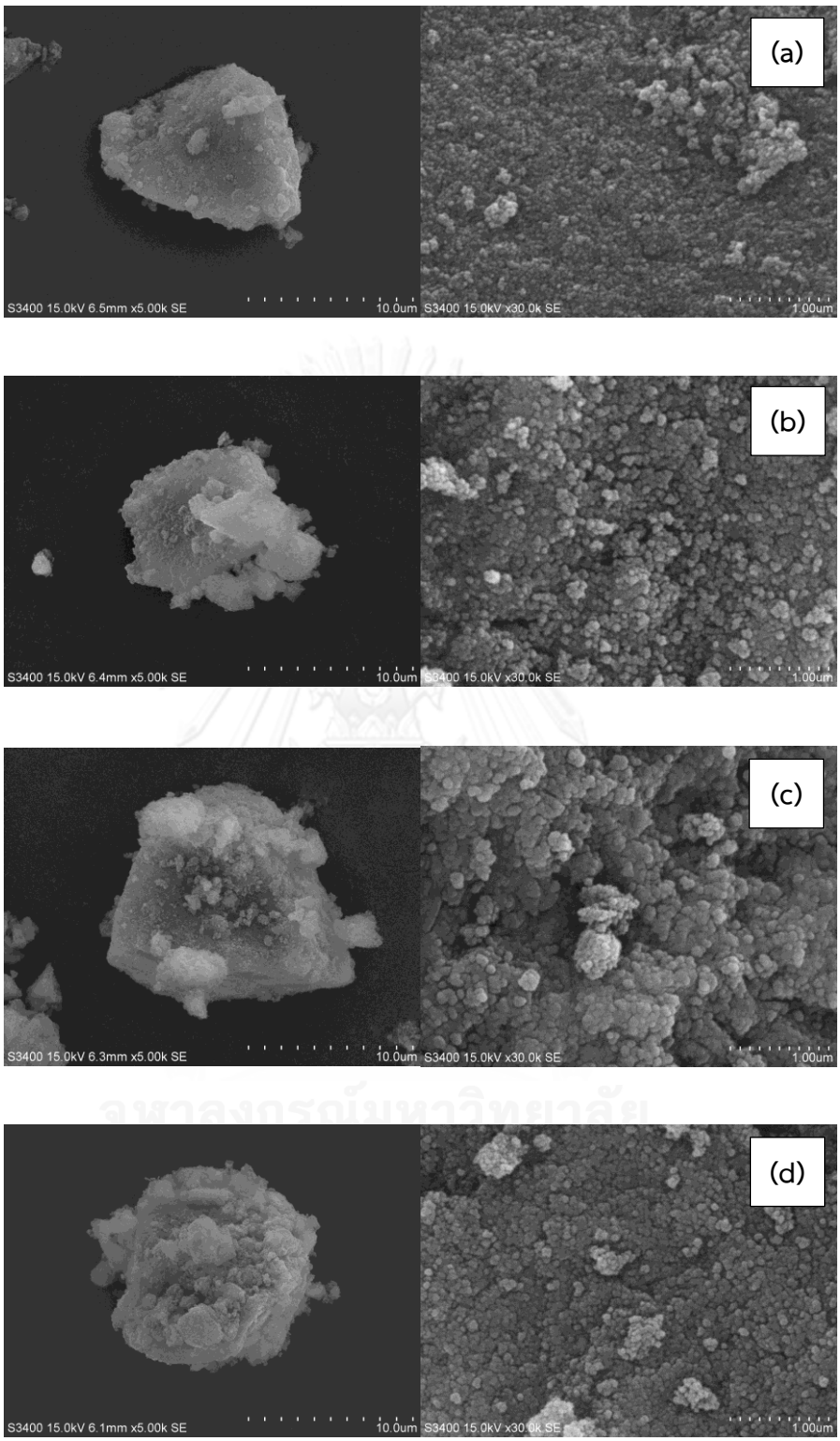

Figure 4.15 SEM micrograph of the MoO_3 over mixed γ- and χ-crystalline phase alumina catalysts with various MoO_3 loading: (a) 5Mo/C50-600, (b) 10Mo/C50-600, (c) 15Mo/C50-600 and (d) 20Mo/C50-600.

Table 4.4 shows the elemental composition over different catalysts detected by EDX. Three components in the catalyst are Al, O, and Mo. Considering the percentage, Al and Owt.% decreased, whereas MoO_3 increased with an increase in MoO_3 loading. The variation of Mo, which was detected by EDX, exhibited nearly the calculating variation. For example, the calculating variation of the 5Mo/C50-600 is 5wt.% while the detected variation by EDX is 6.43wt.%. Nevertheless, the 20Mo/C50-600 shows the variation by EDX (18.88wt.%) lower than the calculating variation (20wt.%). Previous studies, Kady et al. reported [41] that the 16wt.% MoO_3 loading or about 4.04 Mo atoms/nm^2 was distributed on the surface of support probably as monolayer. Therefore, this result can be ascribed to amount of Mo loading to exceeding monolayer content, which may block the pore on surface or attach into the pore, so the detected value is lower than the calculating variation. Moreover, the EDX has limit detection about 5 micron from the surface, which cannot detect deep MoO_3 in the pore.

Table 4.4 EDX component of the MoO_3 over mixed γ- and χ-crystalline phase alumina catalysts with various MoO_3 loading.

Sample	% Weight			% Atom		
	O	Al	Mo	O	Al	Mo
5Mo/C50-600	44.05	49.52	6.43	59.14	39.42	1.44
10Mo/C50-600	43.19	45.83	10.98	59.82	37.64	2.54
15Mo/C50-600	40.86	41.42	17.72	59.76	35.92	4.32
20Mo/C50-600	40.45	40.67	18.88	59.74	35.61	4.65

Figure 4.16 shows elemental dispersion of all catalysts (Al, O, and Mo). The result reveals that all components were well dispersed. The Mo component of all catalysts exhibited good dispersion even though the MoO_3 was added about 20wt.%.

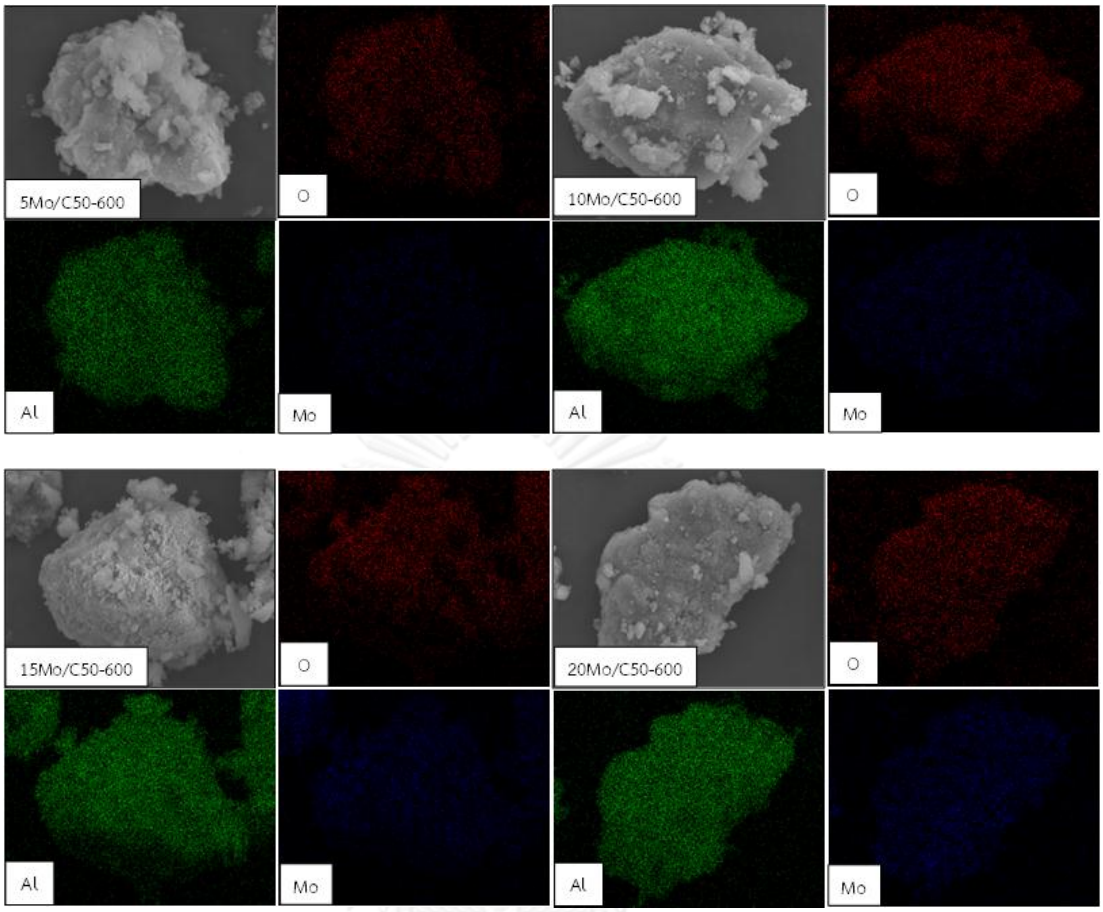

Figure 4.16 Characteristic dispersion of component of the MoO_3 over mixed γ- and χ-crystalline phase alumina catalysts with various MoO_3 loading.

4.2.1.4 Temperature programmed adsorption (NH_3-TPD)

The acidic property of the MoO_3 over different catalyst was investigated by NH_3-TPD. As can be seen in **Figure 4.17**, TPD profiles of all catalysts were similar to C50-600 observed in mixed phase alumina catalysts. The TPD profile can be divided into two peaks, weak acid sites (100-230°C) and medium to strong acid sites (250-500°C). Upon the introduction of MoO_3 added enhancement, it can be seen the TPD profile was shifted to high temperature and TCD signal intensity was increased. It means that the incorporation of MoO_3 on surface catalyst causes the generation of medium to strong acid sites and increases total acidity (661μmol NH_3/g

cat. for the C50-600 compared to 923μmol NH_3/g cat. for the 5Mo/C50-600). The amounts of acidity are shown in **Table 4.5.**

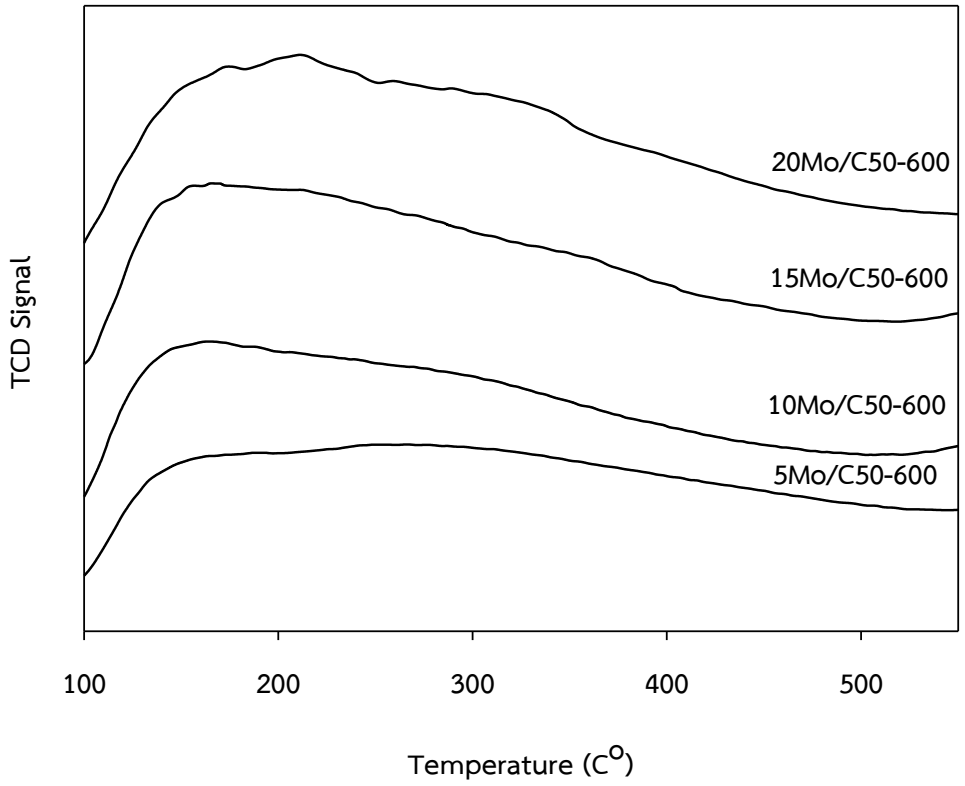

Figure 4.17 NH_3-TPD profiles of the MoO_3 over mixed γ- and χ-crystalline phase alumina catalysts with various MoO_3 loading.

Table 4.2 demonstrates the results of the acidity with different MoO_3 loading. It was found that the total acidity was enhanced explicitly with an increase in the MoO_3 loading, especially the medium to strong acid sites (634μmol NH_3/g cat. for the 5Mo/C50-600 compare to 851μmol NH_3/g cat. for the 20Mo/C50-600). This implies that the addition of MoO_3 has an effect on the acidity of the mixed phase alumina catalysts. Although, the increased acidity with the MoO_3 loading cannot be identified in terms of Lewis and Brønsted acidity, Heracleous et al. [42] suggest that the new acid sites generated from the introduction of Mo are of

Brønsted sprcies, while only Lewis acid sites were identified on the alumina support [26, 43, 44].

Table 4.5 The amount of acidity of the MoO_3 over mixed γ- and χ-crystalline phase alumina catalysts with various MoO_3 loading.

Sample	NH_3 desorption (μmol NH_3/g cat.)		Total acidity (μmol NH_3/g cat.)
	Weak	Medium to strong	
5Mo/C50-600	289	634	923
10Mo/C50-600	249	727	977
15Mo/C50-600	220	795	1015
20Mo/C50-600	263	851	1114

4.2.2 Catalytic activity

From section 4.1, the suitable catalyst was the C50-600. It shows the best catalytic performance in both for the highest ethanol conversion and ethylene selectivity. Therefore, the aim of this part is to investigate an improvement of acidity. So the MoO_3 was interesting in this reaction due to previous literature. We expect that MoO_3 may help to promote acidity of the mixed γ- and χ-crystalline phase alumina catalysts.

The MoO_3 over mixed phase alumina catalysts with various MoO_3 loading from 5wt.% to 20wt.% were tested in ethanol dehydration reaction. The selectivity of ethylene, DEE, and acetaldehyde of all catalysts are shown in **Figure 4.18-4.20**, respectively. Both ethylene and DEE selectivities showed the same trend as the mixed phase alumina catalysts. As ethylene favors high temperature, the DEE requires lower temperature. An enhancement in acetaldehyde selectivity was observed when introducing MoO_3. The increase in selectivity of acetaldehyde was due to the fact that Mo species is promoted dehydrogenation pathway [50]. The

MoO_3 added into the mixed phase alumina substituted the acid sites on catalyst surface, resulting in the new acid sites that were generated. This result is corresponded to NH_3-TPD data, which explained that the acidity on surface of catalysts consists of two type (conventional acid sites and new acid sites form Mo species). It can be implied that ethylene and DEE were produced from conventional acid sites on catalyst surface, whereas the acetaldehyde results from dehydrogenation reaction generates from acid site form Mo species.

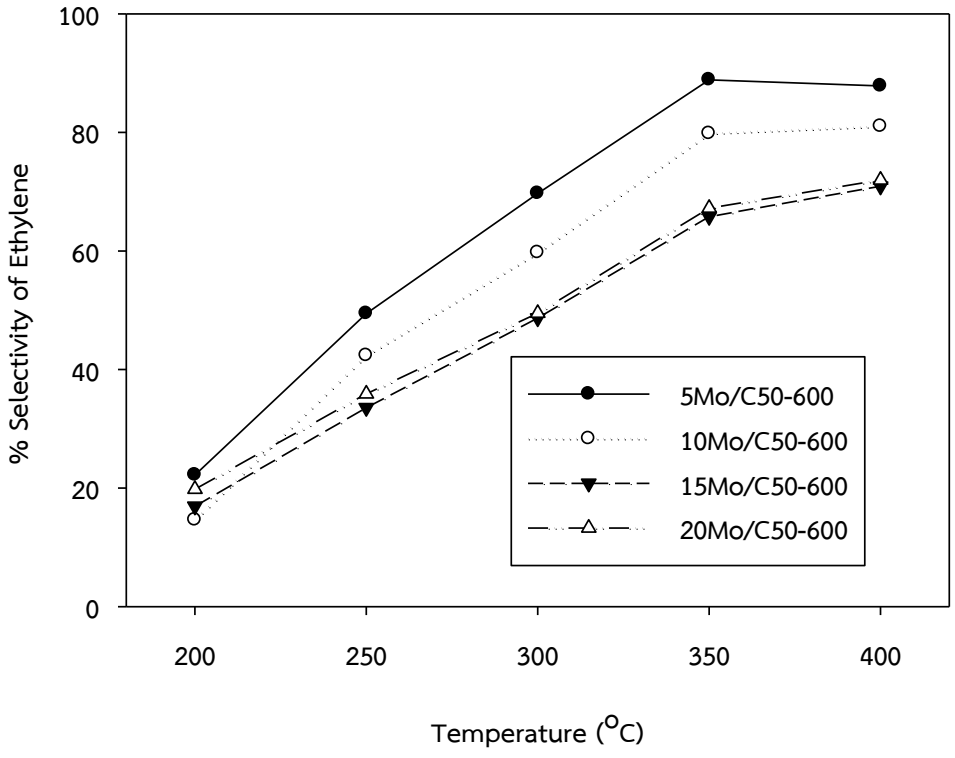

Figure 4.18 Selectivity of ethylene profiles in ethanol dehydration at different temperatures.

The selectivity of ethylene was decreased with an increase of MoO_3 loading. It was in the order of 5Mo/C50-600 > 10Mo/C50-600 > 20Mo/C50-600 > 15Mo/C50-600 as shown in **Figure 4.18.** In contrast, the selectivity of acetaldehyde was increased with an increase of MoO_3 loading. The result was in the order of

15Mo/C50-600 > 20Mo/C50-600 > 10Mo/C50-600 > 5Mo/C50-600 as shown in **Figure 4.19.** Although, the 20Mo/C50-600 exhibits higher amount of the MoO_3 than the 15Mo/C50-600, the selectivity of ethylene is not the lowest or the selectivity of acetaldehyde is not the highest. This was due to the fact that accumulation in catalyst pores was observed when loading MoO_3 over 15wt.%. Thus, it leads to loss of Mo species.

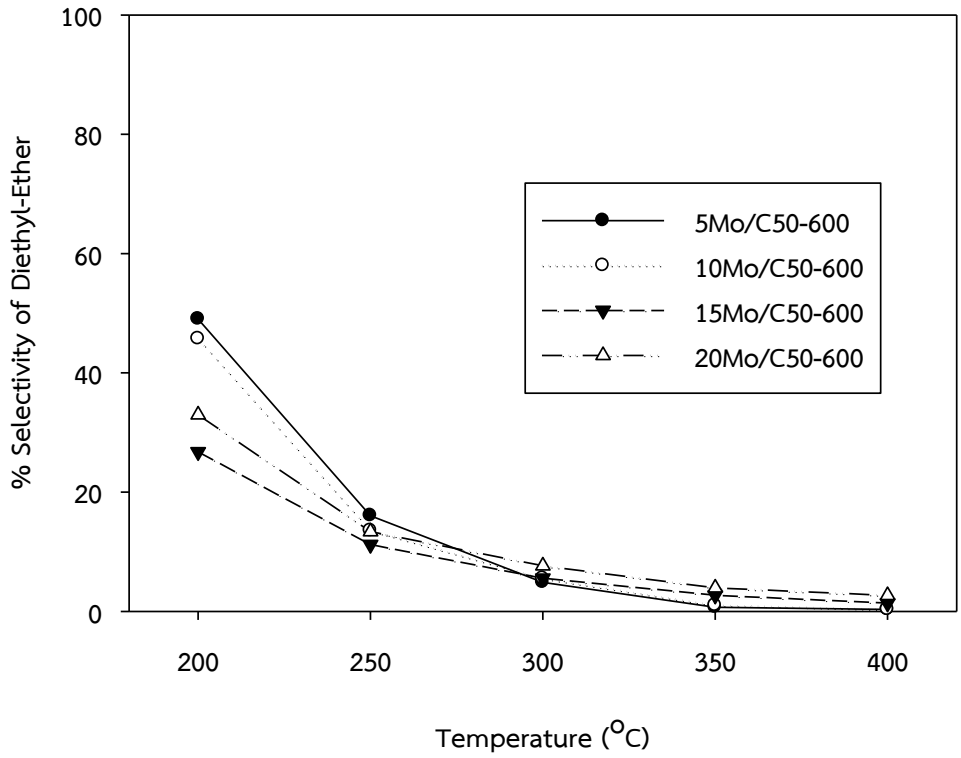

Figure 4.19 Selectivity of DEE profiles in ethanol dehydration at different temperatures.

For the selectivity of ethylene, the 5Mo/C50-600 exhibited the highest ethylene selectivity (88.85% selectivity of ethylene at 350°C). However, it was lower compared to the C50-600 (98.76% selectivity of ethylene at 350°C). The 15Mo/C50-600 had the highest selectivity of acetaldehyde and the selectivity of acetaldehyde was enhanced up to 56.35% at 200°C.

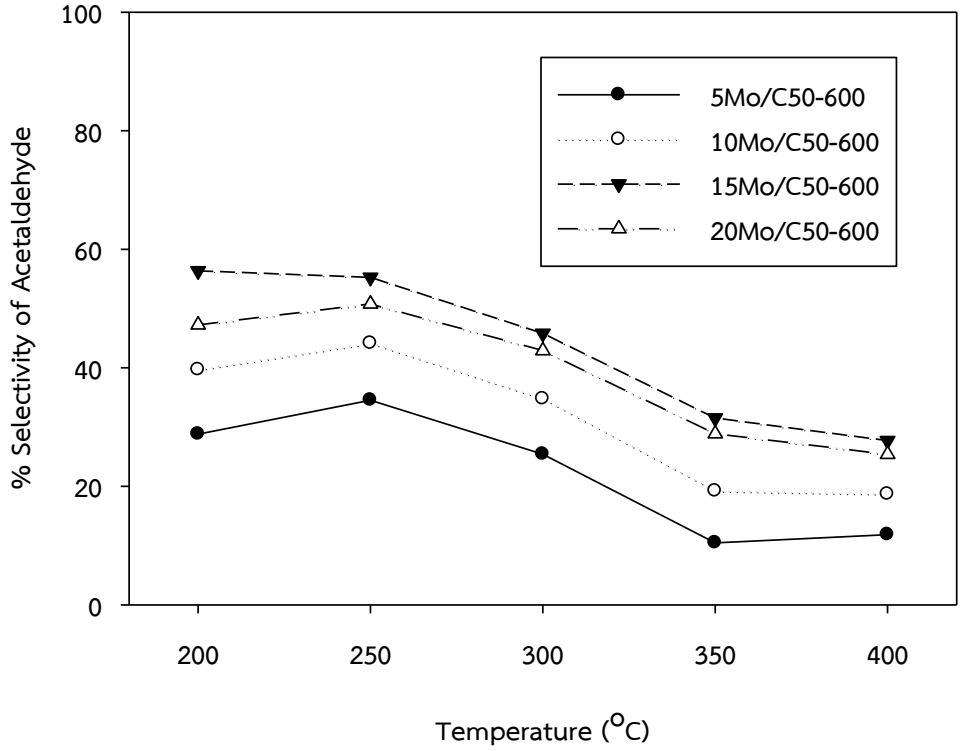

Figure 4.20 Selectivity of acetaldehyde profiles in ethanol dehydration at different temperatures.

The ethanol conversions over different catalysts are shown in **Figure 4.21.** It displays the similar trend to the ethanol conversion of the C50-600, increasing with increase in operating temperatures. When compared the MoO_3 modified alumina series with the unmodified catalysts (C50-600), it was found that the ethanol conversion of modified alumina was lower than that of the C50-600, although the modified alumina had an amount of acidity more than the C50-600 catalyst. For example, the 5Mo/C50-600 exhibited 47.86% ethanol conversion at 200°C, while the C50-600 showed 64.38% ethanol conversion at 200°C. The reason why the higher total acidity did not contribute to the increasing ethanol conversion was attributed to Mo species.

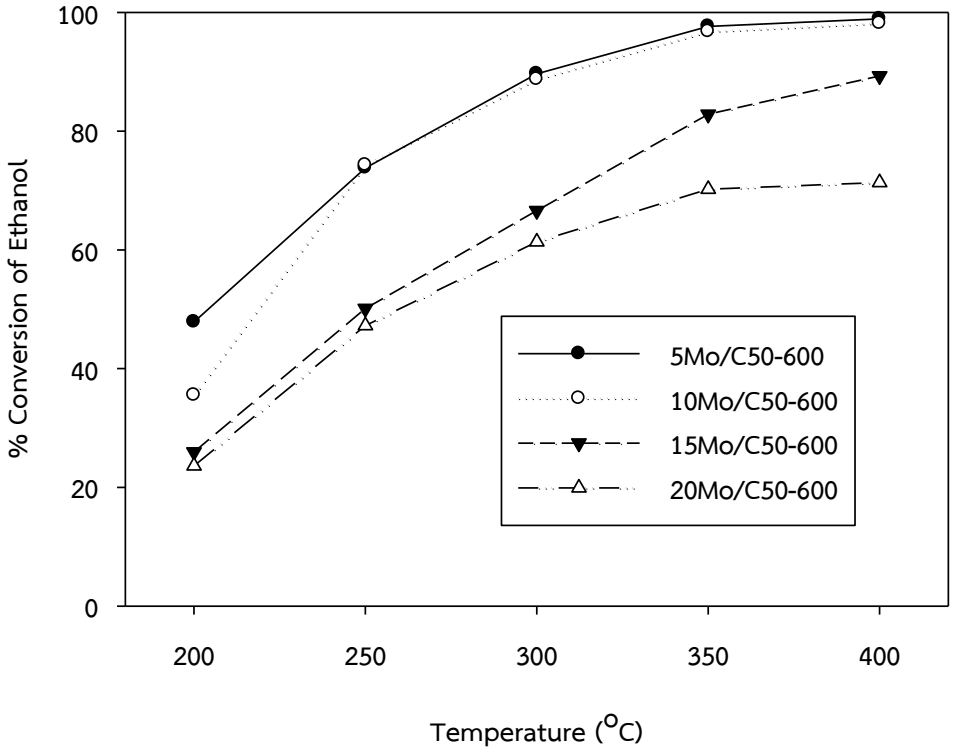

Figure 4.21 Ethanol conversion profiles in ethanol dehydration of the MoO_3 over mixed γ- and χ-crystalline phase alumina catalysts.

Thus, we set up the hypothesis in order to describe this phenomenon as followed in **Scheme 1**.

Hypothesis: the acid site converts the ethanol molecule faster than the Mo site, results in ethanol consumption (1)>(2).

From **Scheme 1**, the catalysts without MoO_3 consist of acid site, act as active phase on surface. While the MoO_3 modified catalysts, some acid sites was taken place by MoO_3. Then, the surface of catalysts actually contains two types of active phase (acid sites and Mo sites). According to previous study, it suggests that the acid site plays an important role for the dehydration reaction (ethanol to ethylene and DEE). Ethanol was consumed very fast by acid site. In contrast, the Mo

sites dominantly acted as the catalysts for the dehydrogenation of ethanol to acetaldehyde. The rate of ethanol consumption was slower than the acid site.

Scheme 1 Ethanol consumption phenomena on active site: EtOH is ethanol, EL is ethylene, DEE is diethyl-ether, and AC is acetaldehyde.

As mentioned above, the ethanol conversion of modified catalyst would cause from the Mo site. To confirm the rate of ethanol consumption by acid site and Mo site, the turnover frequency (TOF) or turnover number, which describes in the molecules reacting per active site in unit time, was calculated as shown in **Table 4.6.**

Table 4.6 Turnover frequency of the acid and Mo sites.

Turnover frequency (s^{-1})	
Acid sites[a]	Mo sites[b]
84.4	4.70×10^{-3}

[a] Based on dehydration reaction of ethanol to ethylene of the C50-600 at 200°C

[b] Based on dehydrogenation reaction of ethanol to acetaldehyde of the 5Mo/C50-600 at 200°C

As can be seen in **Table 4.6,** the TOF of acid site was $84.4 s^{-1}$. It means that the 84.4 ethanol molecules were converted to ethylene on each acid site per second. Similarity, the 4.70×10^{-3} ethanol molecules converted to acetaldehyde on each Mo site per second. The TOF of acid sites was higher than that of Mo sites.

Therefore, when the MoO_3 was added, the acid site and generated new sites (Mo sites) were formed in catalyst. The Mo slowly converted the ethanol molecule resulted in decreasing overall ethanol consumption.

CHAPTER V

CONCLUSIONS AND RECOMMENDATIONS

In this research, we study in characteristic and catalytic activity of the mixed γ- and χ-crystalline phase alumina catalysts, which is considered in the effect of calcination temperature and metal oxide loading in order to clear up in ethanol dehydration reaction. Also, this chapter is summarized the results overall study in section 5.1 and the recommendations about this research in section 5.2.

5.1 Conclusions

1. The calcination temperature above 1000°C of the mixed γ- and χ-crystalline phase alumina catalysts significantly affects on phase transform. The γ-phase was changed while the χ- phase remains stable.

2. The calcination temperature and metal oxide loading have an effect on acidity.

   - The acidity was decreased with increasing calcination temperature.
   - The acidity was increased with increasing metal oxide loading especially medium to strong acid.

3. Both ethanol conversion and ethylene selectivity of ethanol dehydration reaction depend on medium to strong acid.

4. The MoO_3 on surface is active sites promoted the dehydrogenation reaction pathway.

5. The suitable catalyst is the C50-600 and it shows highest catalytic activity, 99.98% ethanol conversion and 98.76% ethylene selectivity at 350°C.

5.2 Recommendations

According to literature reviews, the acidity significantly affects on catalytic activity of ethanol dehydration reaction. Therefore, this research was emphasized the effect of acidity by using NH_3-TPD. However, there are several techniqes for investigation and several effects for study in order to better understanding this reaction. Thus, we propose recommendation as follows:

- To indicated type of acidity (Bronsted and Lewis) with Infrared spectrophotometer (FTIR).

- To consider on life span and stability of the C50-600 with constant reaction temperature.

- To study coke formation and investigated how to reduce coke formation.

In order to apply for industry, we should use different sources of reactant (ethanol).

REFERENCES

[1] Bedia, J., Barrionuevo, R., Rodríguez-Mirasol, J., and Cordero, T. Ethanol dehydration to ethylene on acid carbon catalysts. Applied Catalysis B: Environmental 103(3) (2011): 302-310.

[2] Zotov, R.A., Molchanov, V.V., Volodin, A.M., and Bedilo, A.F. Characterization of the active sites on the surface of Al_2O_3 ethanol dehydration catalysts by EPR using spin probes. Journal of Catalysis 278(1) (2011): 71-77.

[3] Fan, D., Dai, D.-J., and Wu, H.-S. Ethylene formation by catalytic dehydration of ethanol with industrial considerations. Materials 6(1) (2012): 101-115.

[4] Zhang, M. and Yu, Y. Dehydration of ethanol to ethylene. Industrial & Engineering Chemistry Research 52(28) (2013): 9505-9514.

[5] Takahashi, A., Xia, W., Nakamura, I., Shimada, H., and Fujitani, T. Effects of added phosphorus on conversion of ethanol to propylene over ZSM-5 catalysts. Applied Catalysis A: General 423 (2012): 162-167.

[6] Lu, J., Liu, Y., and Li, N. Fe-modified HZSM-5 catalysts for ethanol conversion into light olefins. Journal of Natural Gas Chemistry 20(4) (2011): 423-427.

[7] Ouyang, J., Kong, F., Su, G., Hu, Y., and Song, Q. Catalytic conversion of bio-ethanol to ethylene over La-modified HZSM-5 catalysts in a bioreactor. Catalysis letters 132(1-2) (2009): 64-74.

[8] Zaki, T. Catalytic dehydration of ethanol using transition metal oxide catalysts. Journal of colloid and Interface Science 284(2) (2005): 606-613.

[9] Chen, G., Li, S., Jiao, F., and Yuan, Q. Catalytic dehydration of bioethanol to ethylene over TiO_2/ γ-Al_2O_3 catalysts in microchannel reactors. Catalysis Today 125(1) (2007): 111-119.

[10] Khom-in, J., Praserthdam, P., Panpranot, J., and Mekasuwandumrong, O. Dehydration of methanol to dimethyl ether over nanocrystalline Al_2O_3 with mixed γ- and χ-crystalline phases. Catalysis Communications 9(10) (2008): 1955-1958.

[11] Khom-in, J. Synthesis of dimethylether (DME) from dehydration of methanol using γ-Al_2O_3 and γ- χ-Al_2O_3 catalysts. Master Degree, Chemical Engineering Chulalongkorn University, 2007.

[12] Pansanga, K., Panpranot, J., Mekasuwandumrong, O., Satayaprasert, C., Goodwin, J.G., and Praserthdam, P. Effect of mixed γ- and χ-crystalline phases in nanocrystalline Al_2O_3 on the dispersion of cobalt on Al_2O_3. Catalysis Communications 9(2) (2008): 207-212.

[13] Meephoka, C., Chaisuk, C., Samparnpiboon, P., and Praserthdam, P. Effect of phase composition between nano γ- and χ-Al_2O_3 on Pt/Al_2O_3 catalyst in CO oxidation. Catalysis Communications 9(4) (2008): 546-550.

[14] Bokade, V.V. and Yadav, G.D. Heteropolyacid supported on montmorillonite catalyst for dehydration of dilute bio-ethanol. Applied Clay Science 53(2) (2011): 263-271.

[15] Varisli, D., Dogu, T., and Dogu, G. Ethylene and diethyl-ether production by dehydration reaction of ethanol over different heteropolyacid catalysts. Chemical Engineering Science 62(18) (2007): 5349-5352.

[16] Nowak, I. and Ziolek, M. Niobium compounds: preparation, characterization, and application in heterogeneous catalysis. Chemical Reviews 99(12) (1999): 3603-3624.

[17] Leroy G. Wade, J. Organic Chemistry. Fifth Edition ed. saddle River, New jersey: prentice-Hall, 2003.

[18] Wittayakhun J., K.N. Catalysis: Fundamentals and Application. 1st ed ed.: Thammasart university 2004.

[19] Cheng, L.-T., Tsai, M.-Y., Tseng, W.J., Hsiang, H.-I., and Yen, F.-S. Boehmite coating on θ-Al_2O_3 particles via a sol–gel route. Ceramics International 34(2) (2008): 337-343.

[20] Li, J., Pan, Y., Xiang, C., Ge, Q., and Guo, J. Low temperature synthesis of ultrafine α-Al_2O_3 powder by a simple aqueous sol–gel process. Ceramics International 32(5) (2006): 587-591.

[21] Somiya, S. Handbook of Advanced Ceramics: Materials, Applications, Processing, and Properties. Academic Press, 2013.

[22] Carrier, X., Lambert, J.-F., Kuba, S., Knözinger, H., and Che, M. Influence of ageing on MoO_3 formation in the preparation of alumina-supported Mo catalysts. Journal of molecular structure 656(1) (2003): 231-238.

[23] Kitano, T., Okazaki, S., Shishido, T., Teramura, K., and Tanaka, T. Brønsted acid generation of alumina-supported molybdenum oxide calcined at high temperatures: Characterization by acid-catalyzed reactions and spectroscopic methods. Journal of Molecular Catalysis A: Chemical 371(0) (2013): 21-28.

[24] Abello, M.C., Gomez, M.F., Casella, M., Ferretti, O.A., Bañares, M.A., and Fierro, J.L.G. Characterization and performance for propane oxidative dehydrogenation of Li-modified MoO_3/Al_2O_3 catalysts. Applied Catalysis A: General 251(2) (2003): 435-447.

[25] Lowenthal, E.E., Schwarz, S., and Foley, H.C. Surface Chemistry of Rh-Mo/γ-$A_{l2}O_3$: An Analysis of Surface Acidity. Journal of Catalysis 156(1) (1995): 96-105.

[26] Han, Y., Lu, C., Xu, D., Zhang, Y., Hu, Y., and Huang, H. Molybdenum oxide modified HZSM-5 catalyst: Surface acidity and catalytic performance for the dehydration of aqueous ethanol. Applied Catalysis A: General 396(1) (2011): 8-13.

[27] R., P.L. Development review of catalysts for ethanol dehydration to produce ethylene. Speciality Petrochem (4) (1986): 41-64.

[28] Pearson, D.E., Tanner, R.D., Picciotto, I.D., Sawyer, J.S., and Cleveland Jr, J.H. Phosphoric acid systems. 2. Catalytic conversion of fermentation ethanol to ethylene. Industrial & Engineering Chemistry Product Research and Development 20(4) (1981): 734-740.

[29] Zhang, D., Wang, R., and Yang, X. Effect of P Content on the Catalytic Performance of P-modified HZSM-5 Catalysts in Dehydration of Ethanol to Ethylene. Catalysis letters 124(3-4) (2008): 384-391.

[30] Ramesh, K., Jie, C., Han, Y.-F., and Borgna, A. Synthesis, characterization, and catalytic activity of phosphorus modified H-ZSM-5 catalysts in selective ethanol dehydration. Industrial & Engineering Chemistry Research 49(9) (2010): 4080-4090.

[31] Hu, Y., et al. Selective dehydration of bio-ethanol to ethylene catalyzed by lanthanum-phosphorous-modified HZSM-5: Influence of the fusel. Biotechnology journal 5(11) (2010): 1186-1191.

[32] Madeira, F.F., Gnep, N., Magnoux, P., Maury, S., and Cadran, N. Ethanol transformation over HFAU, HBEA and HMFI zeolites presenting similar Brønsted acidity. Applied Catalysis A: General 367(1) (2009): 39-46.

[33] Zhan, N., Hu, Y., Li, H., Yu, D., Han, Y., and Huang, H. Lanthanum–phosphorous modified HZSM-5 catalysts in dehydration of ethanol to ethylene: A comparative analysis. Catalysis Communications 11(7) (2010): 633-637.

[34] Matachowski, L., Zimowska, M., Mucha, D., and Machej, T. Ecofriendly production of ethylene by dehydration of ethanol over $Ag_3PW_{12}O_{40}$ salt in nitrogen and air atmospheres. Applied Catalysis B: Environmental 123 (2012): 448-456.

[35] Hernández-Cortez, J., Manríquez, M., Lartundo-Rojas, L., and López-Salinas, E. Study of acid–base properties of supported heteropoly acids in the reactions of secondary alcohols dehydration. Catalysis Today 220 (2014): 32-38.

[36] Kwak, J.H., Mei, D., Peden, C.H., Rousseau, R., and Szanyi, J. (100) facets of γ-Al_2O_3: The Active Surfaces for Alcohol Dehydration Reactions. Catalysis letters 141(5) (2011): 649-655.

[37] Santacesaria, E., Gelosa, D., and Carrà, S. Basic behavior of alumina in the presence of strong acids. Industrial & Engineering Chemistry Product Research and Development 16(1) (1977): 45-47.

[38] Ros, S.D., Barbosa-Coutinho, E., Schwaab, M., Calsavara, V., and Fernandes-Machado, N.R. Modeling the effects of calcination conditions on the physical and chemical properties of transition alumina catalysts. Materials Characterization 80 (2013): 50-61.

[39] Shishido, T., Kitano, T., Teramura, K., and Tanaka, T. Generation of brönsted acid over alumina-supported niobia calcined at high temperatures. Topics in Catalysis 53(7-10) (2010): 672-677.

[40] Webster, T.J., Hellenmeyer, E.L., and Price, R.L. Increased osteoblast functions on theta+ delta nanofiber alumina. Biomaterials 26(9) (2005): 953-960.

[41] El Kady, F., Shaban, S., and El Naga, A.A. Catalytic dehydrogenation of cyclohexene over MoO_3/γ-Al_2O_3 catalysts. Transition Metal Chemistry 36(2) (2011): 237-244.

[42] Heracleous, E., Lemonidou, A.A., and Lercher, J.A. Mechanistic features of the ethane oxidative dehydrogenation by in situ FTIR spectroscopy over a MoO_3/Al_2O_3 catalyst. Applied Catalysis A: General 264(1) (2004): 73-80.

[43] Heracleous, E., Lee, A., Vasalos, I., and Lemonidou, A. Surface properties and reactivity of Al_2O_3-supported MoO_3 catalysts in ethane oxidative dehydrogenation. Catalysis letters 88(1-2) (2003): 47-53.

[44] Kiviat, F. and Petrakis, L. Surface acidity of transition metal modified aluminas. Infrared and nuclear magnetic resonance investigation of adsorbed pyridine. The Journal of Physical Chemistry 77(10) (1973): 1232-1239.

APPENDICES

APPANDIX A

CONVERSION AND SELECTIVITY

Calculation of molybdenum oxide loading

The MoO_3 modified mixed phase alumina catalysts were prepared by impregnation of mixed phase alumina with an aqueous solution of ammonium heptamolybdate-tetrahydat (AHM). The preparation catalyst was calculated based on 1g of catalyst used.

For example, the 5Mo/C50-600 was prepared as follow:

Based on 1g of catalyst used, the 5Mo/C50-600 catalyst contain 5wt.% of Mo. So the catalyst composition would be as follow:

Molybdenum	=	0.05g
C50-600	=	1.00-0.05g
	=	0.95g

Reagent data: - Ammonium heptamolybdate-tetrahydrat $[(NH_4)_6Mo_7O_{24}\bullet 4H_2O]$
Molecular weight = 1,236.01g/mol
- Molybdenum (Mo), atomic weight = 95.96g/mol
- Support : C50-600

AHM formula is consisted of 7 Mo atom so weigh of Mo in AHM is 671.72g (95.96x7).

Mo	671.72g	in AHM	1,236.01g
Mo	0.05g	in AHM	1,236.01x0.05/671.72g
			= 0.092g

APPANDIX B

CALIBRATION CURVE

Calibration curves were used calculation mole of ethanol, ethylene, DEE and acetaldehyde as shown in **Figure B.1-B.4**. The concentration of these were analyzed by the gas chromatography Shimadzu model 14A, capillary column DB-5 of flame ionization detector (FID). The conditions uses in GC are presented in **Table B.1**

Table B.1 Conditions use in GC-14A.

Parameters	Condition
Width	5
Slope	100
Drift	0
Min.area	300
T.DBL	1000
Stop time	12 min
Atten	2
Speed	3
Method	Normalization
SPL.WT	100
IS.WT	1

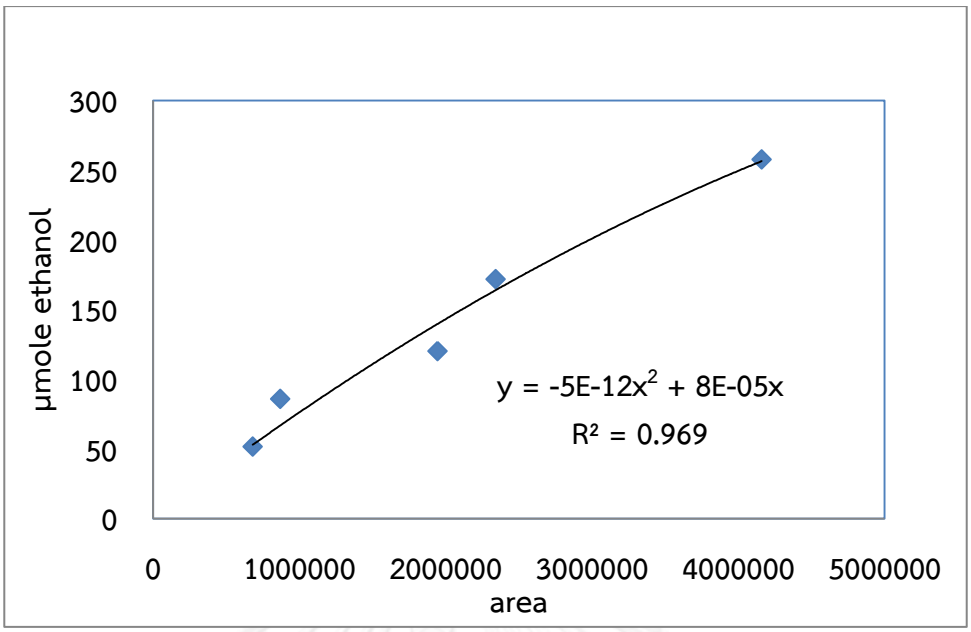

Figure B.1 The calibration curve of ethanol.

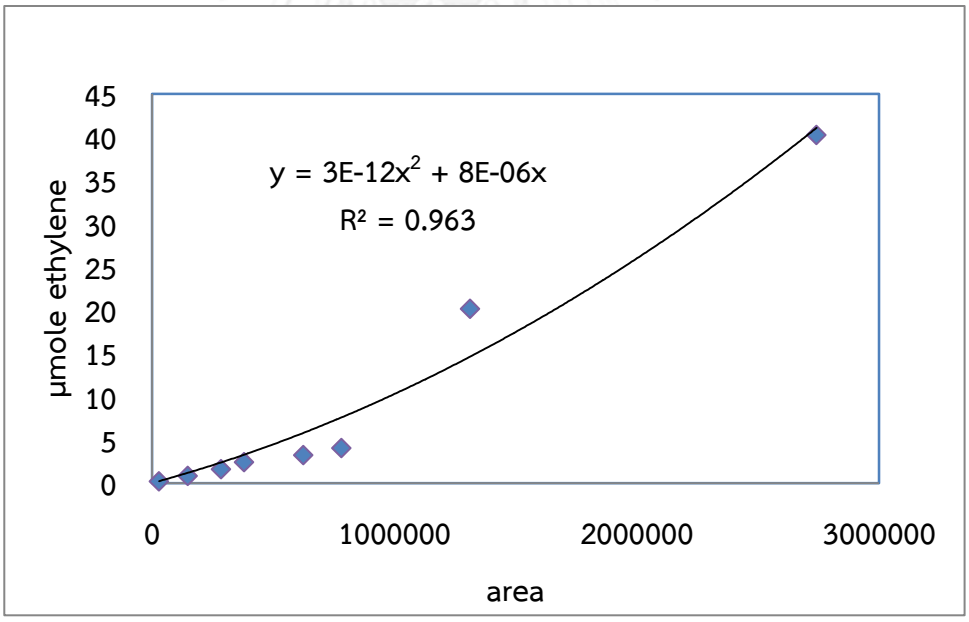

Figure B.2 The calibration curve of ethylene.

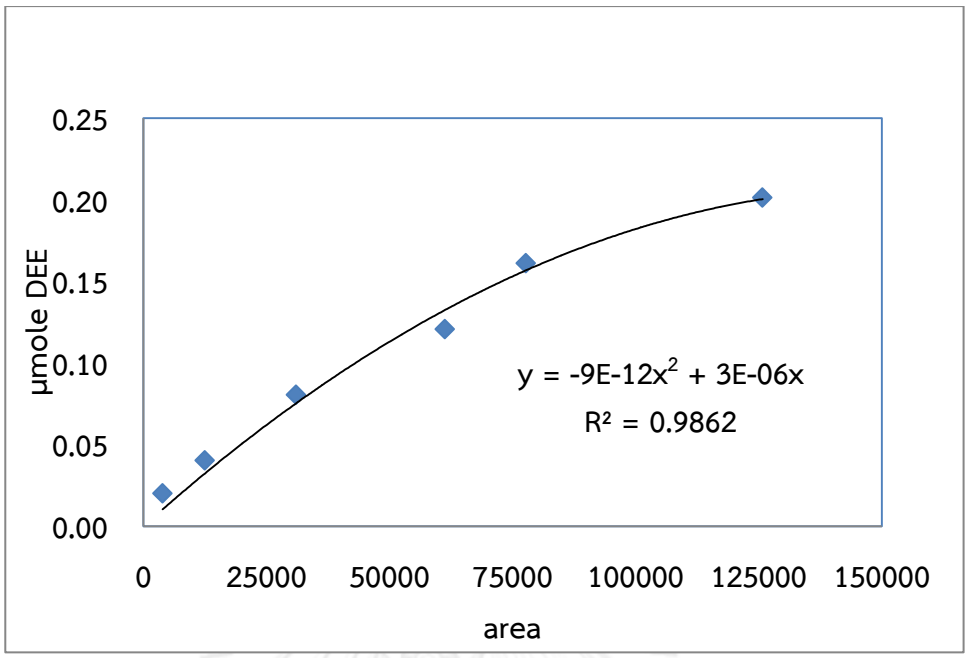

Figure B.3 The calibration curve of DEE.

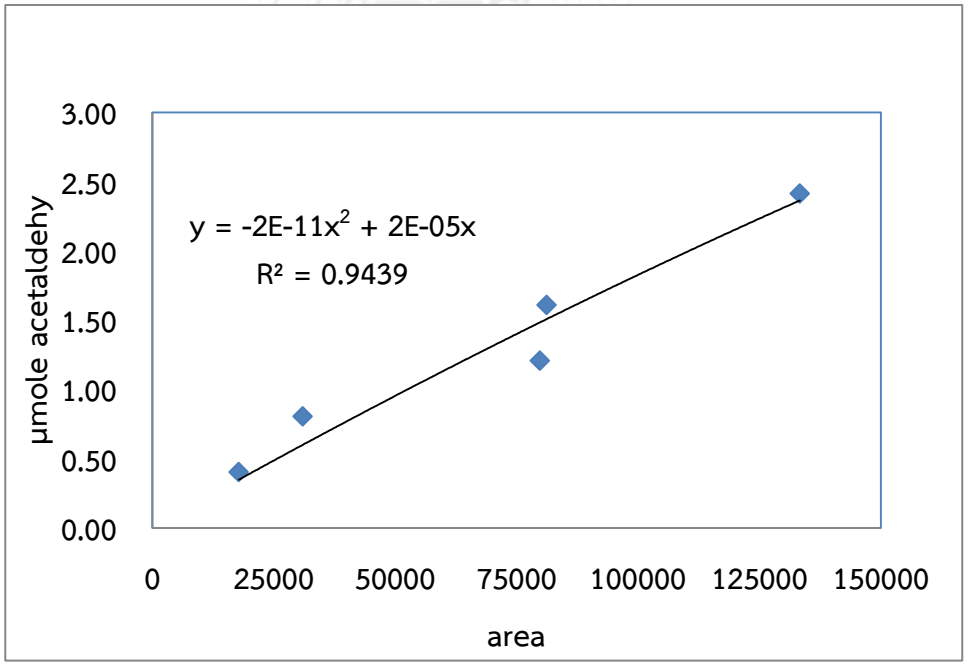

Figure B.4 The calibration curve of acetaldehyde.

APPANDIX C

CONVERSION AND SELECTIVITY

C.1 Ethanol conversion

$$\text{EtOH conversion (\%)} = \frac{[\text{EtOH in (mole)} - \text{EtOH out (mole)}]}{[\text{EtOH in (mole)}]} \times 100$$

C.2 Selectivity of product

$$\text{A selectivity (\%)} = \frac{[\text{A in product (mole)}]}{[\text{Total product (mole)}]} \times 100$$

Where: A is mole of Ethylene, DEE, or Acetaldehyde.

Total product is mole of (Ethylene + DEE + Acetaldehyde).

APPANDIX D

CALCULATION OF ACIDITY

Calculation of acidity

The acidity was measured by NH_3-TPD, it can be calculated from NH_3-TPD profile as equation (D.1)

$$\text{Acidity of catalysts} = \frac{[\text{mole of } NH_3 \text{ desorption}]}{[\text{amount of dry catalyst}]} \qquad \text{equation (D.1)}$$

To Calculate mole of NH_3 desorption from the calibration curve of NH_3 as follow:

$$NH_3 \text{ desorption (mole)} = 0.0003 \times A$$

Where, A is area under peak of the NH_3-TPD profile.

And then, we denote amount of dry catalyst as B (g.). So the equation (D.1) can be take place as equation (D.2)

$$\text{Acidity of catalysts} = \frac{[0.0003 \times A]}{[B]} \qquad \text{equation (D.2)}$$

APPANDIX E

REACTION RATE AND TURNOVER FREQUENCY

E.1 Reaction rate

The ethanol dehydration was obtained several products. There are investigated 3 products (ethylene, DEE, and acetaldehyde). The chemical reaction of each product is shown in equation (E.1), (E.2), and (E.3) as follows:

$C_2H_5OH \longrightarrow C_2H_4 + H_2O$ equation (E.1)

$2\ C_2H_5OH \longrightarrow C_4H_{10}O + H_2O$ equation (E.2)

$C_2H_5OH \longrightarrow C_2H_4O + H_2$ equation (E.3)

From the chemical reaction, the reaction rate is defined as:

$$-r_{E(E.1)} = +r_{ET}$$

$$-r_{E(E.2)} = +2r_{DEE}$$

$$-r_{E(E.3)} = +r_{AC}$$

Where: r_E = rate of ethanol

r_{ET} = rate of ethylene

r_{DEE} = rate of diethyl ether

r_{AC} = rate of acetaldehyde

Therefore, the rate total of ethanol consumption can be written as shown below.

$$-r_E = r_{ET} + 2r_{DEE} + r_{AC}$$

Where the reaction rate of each substance had given in unit of $\frac{\mu mole}{h.\ g.cat}$

So, the reaction rate was calculated as formula:

$$rate = X \frac{\mu mole}{ml} \times Y \frac{ml}{min} \times 60 \frac{min}{h} \times \frac{1}{Z\ g.cat}$$

Where: X = mole of substance per ml

Y = flow rate

Z = amount of catalysts

For example:

Using 0.05g. of the 5M/C50-600 was tested for ethanol dehydration at 200°C with ethanol feed 50ml/min, 0.113μmole ethylene can be detected by GC with 1ml sampling.

Then,

$$r_{Ethylene} = 0.113 \frac{\mu mole}{ml} \times 50 \frac{ml}{min} \times 60 \frac{min}{h} \times \frac{1}{0.05g.cat}$$

$$= 6.79 \times 10^{3} \frac{\mu mole}{h.\ g.cat}$$

E.2 Turnover frequency

Turnover frequency (TOF) in catalysis commonly called the turnover number (N), as molecules reacting per active site in unit time. The TOF of A can be derived as the following.

$$TOF\ (s^{-1}) = \frac{rate_A \times (6.02 \times 10^{23})}{molecule\ of\ active\ sites}$$

$$= \frac{\text{rate}_A \times (6.02 \times 10^{23})}{\mu\text{mole of active sites} \times (6.02 \times 10^{23})}$$

$$= \frac{\text{rate}_A}{\mu\text{mole of active sites}}$$

In this thesis, we was investigated the TOF of ethylene, DEE and acetaldehyde. From previous study, it suggest that the ethanol was converted to ethylene by medium to strong acid sites, converted to DEE by weak acid sites, and converted to acetaldehyde by redox sites (Mo sites). Also, the TOF of these can be written the equation as shown

$$TOF_{Ethylene} = \frac{\text{rate}_{Ethylene}}{\mu\text{mole of medium to strong acid}}$$

$$TOF_{DEE} = \frac{\text{rate}_{DEE}}{\mu\text{mole of weak acid sites}}$$

$$TOF_{Acetaldehyde} = \frac{\text{rate}_{Acetaldehyd}}{\mu\text{mole of Mo sites}}$$

Where the μmole of medium to strong and weak acid sites are acquired form NH_3-TPD technique, assuming all acid sites are dehydrate site. The μmole of Mo sites is acquired form EDX technique, assuming Mo sites is dehydrogenate site.

The TOF of all product are summarized in **Table E.1** to **E.6**

Table E.1 the TOF of ethanol (ET) and diethylether (DEE) of the C50-600.

Temperature (°C)	Products (μmol)		Rate (μmol/h g.cat)		TOF* (s^{-1})	
	ET	DEE	ET	DEE	ET	DEE
200	0.72	1.76×10^{-1}	4.32×10^{4}	1.06×10^{4}	84.4	20.6
250	3.56	1.07×10^{-1}	2.14×10^{5}	6.43×10^{3}	417	12.5
300	3.98	1.22×10^{-3}	2.39×10^{5}	$7.33 \times x10^{1}$	465	0.14
350	3.91	2.77×10^{-4}	2.35×10^{5}	1.66×10^{1}	458	0.03
400	3.67	4.20×10^{-3}	2.20×10^{5}	2.52×10^{2}	430	0.49

*The medium to strong and weak acid sites by NH_3-TPD technique are 513 and 148 μmole, respectively.

Table E.2 the TOF of ethanol (ET) and diethylether (DEE) of the C50-500.

Temperature (°C)	Products (μmol)		Rate (μmol/h g.cat)		TOF* (s^{-1})	
	ET	DEE	ET	DEE	ET	DEE
200	0.76	2.05×10^{-1}	4.56×10^{4}	1.23×10^{4}	84.6	87.8
250	2.99	2.08×10^{-1}	1.80×10^{5}	1.37×10^{3}	333	97.6
300	3.96	2.11×10^{-3}	2.38×10^{5}	$1.27 \times x10^{1}$	440	0.94
350	4.18	4.85×10^{-4}	2.51×10^{5}	2.91×10^{1}	465	0.20
400	4.03	3.33×10^{-3}	2.42×10^{5}	2.00×10^{2}	448	1.43

*The medium to strong and weak acid sites by NH_3-TPD technique are 539 and 140μmole, respectively.

Table E.3 the TOF of acetaldehyde of the the 5M/C50-600

Temperature (°C)	Product (μmol)	Rate (μmol/h g.cat)	TOF* (s^{-1})
	AC	AC	AC
200	0.15	1.40×10^{-1}	4.70×10^{-3}
250	0.54	3.23×10^{4}	1.72×10^{-2}
300	0.73	4.35×10^{4}	2.32×10^{-2}
350	0.33	1.96×10^{4}	1.05×10^{-2}
400	0.37	2.20×10^{4}	1.18×10^{-2}

*The Mo was detected by EDX technique is 6.43wt.%

Table E.4 the TOF of acetaldehyde of the the 10M/C50-600

Temperature (°C)	Product (μmol)	Rate (μmol/h g.cat)	TOF* (s^{-1})
	AC	AC	AC
200	0.21685	1.30×10^{4}	3.16×10^{-3}
250	0.747269	4.48×10^{4}	1.09×10^{-2}
300	1.185338	7.11×10^{4}	1.73×10^{-2}
350	0.733818	4.40×10^{4}	1.07×10^{-2}
400	0.672537	4.04×10^{4}	9.80×10^{-2}

*The Mo was detected by EDX technique is 10.98wt.%

Table E.5 the TOF of acetaldehyde of the 15M/C50-600

Temperature (°C)	Product (μmol)	Rate (μmol/h g.cat)	TOF* (s^{-1})
	AC	AC	AC
200	0.34	2.05×10^{4}	3.09×10^{-3}
250	0.95	5.71×10^{4}	8.59×10^{-3}
300	1.23	7.40×10^{4}	1.11×10^{-2}
350	1.02	6.31×10^{4}	9.22×10^{-3}
400	0.93	5.61×10^{4}	8.44×10^{-3}

*The Mo was detected by EDX technique is 17.72wt.%

Table E.6 the TOF of acetaldehyde of the 20M/C50-600

Temperature (°C)	Product (μmol)	Rate (μmol/h g.cat)	TOF* (s^{-1})
	AC	AC	AC
200	0.28	1.71×10^{4}	2.41×10^{-3}
250	0.84	5.05×10^{4}	7.13×10^{-3}
300	1.03	6.18×10^{4}	8.73×10^{-3}
350	0.76	4.55×10^{4}	6.43×10^{-3}
400	0.68	4.06×10^{4}	5.73×10^{-3}

*The Mo was detected by EDX technique is 18.88wt.%

APPANDIX F

LIST OF PUBLICATION

Proceeding

Tharmmanoon Inmanee and Bunjerd jongsomjit, “The Effect of Calcination Temperatures for Mixed Phases Al_2O_3 on Ethanol Dehydration Reaction.” Proceeding of the 23rd TiChE national Conference 2013, Khon Kaen University, Thailand, October 17-18, 2013.

VITA

Mr. Tharmmanoon Inmanee was born on DEC10, 1989 in Nakhon Sawan, Thailand. He recived the Bachelor's Degree in Chemical Engineering from the Department of Chemical Engineering, Faculty of Engineering, Srinakharinwirot University (SWU) in May 2012. He continued the Master of Engineering in Chemical Engineering, Chulalongkorn University (CU) in June 2012.